NATIONAL ADVISORY COMMITTEE FOR AERONAUTICS

MAY 2 1947
TECHNICAL NOTE

No. 1270

EXPERIMENTAL AND CALCULATED CHARACTERISTICS OF SEVERAL NACA 44-SERIES WINGS WITH ASPECT RATIOS OF 8, 10, AND 12 AND TAPER RATIOS OF 2.5 AND 3.5

By Robert H. Neely, Thomas V. Bollech,
Gertrude C. Westrick, and Robert R. Graham

Langley Memorial Aeronautical Laboratory
Langley Field, Va.

Washington

May 1947

NATIONAL ADVISORY COMMITTEE FOR AERONAUTICS

TECHNICAL NOTE NO. 1270

EXPERIMENTAL AND CALCULATED CHARACTERISTICS OF SEVERAL NACA 44-SERIES WINGS WITH ASPECT RATIOS OF 8, 10, AND 12 AND TAPER RATIOS OF 2.5 AND 3.5

By Robert H. Neely, Thomas V. Bollech, Gertrude C. Westrick, and Robert R. Graham

SUMMARY

The aerodynamic characteristics of seven unswept tapered wings were determined by calculation from two-dimensional data and by wind-tunnel tests in order to demonstrate the accuracy of the calculations and to show some of the effects of aspect ratio, taper ratio, and root thickness-chord ratio. The characteristics were calculated by the usual application of the lifting-line theory which assumes linear section lift curves and also by an application of the theory which allows the use of nonlinear lift curves. A correction to the lift for the effect of chord was made by using the Jones edge-velocity factor. The wings had aspect ratios of 8, 10, and 12, taper ratios of 2.5 and 3.5, and NACA 44-series airfoils. For six of the wings the ratio of span to root thickness was held constant at 35 so that the root thickness-chord ratio increased with increasing aspect ratio. The aerodynamic characteristics of the wings with and without leading-edge roughness are presented for small values of Mach number and values of Reynolds number between 1.5×10^6 and 7.0×10^6.

Reasonable agreement was obtained between the wing force and moment characteristics calculated by the two methods and those obtained experimentally; however, the method of calculation which allowed the use of nonlinear lift curves gave better agreement at high angles of attack. The two methods of calculation gave different spanwise lift distributions at maximum lift. Comparisons made at equal values of Reynolds number indicate that the values of the maximum lift-drag ratio $(L/D)_{max}$ of the smooth wings increased with increasing aspect ratio throughout the range investigated in spite of the increased drag of the thicker root sections associated with the higher aspect ratios. The values of $(L/D)_{max}$ for the wings of taper ratio 3.5 with leading-edge roughness indicated the same trend; however, the values for the wings of taper ratio 2.5 with leading-edge roughness

showed no gain when the aspect ratio was increased from 10 to 12, apparently because of the larger increment of profile drag due to roughness on the thicker root sections of the wing of aspect ratio 12. The decrement in $(L/D)_{max}$ due to roughness was considerably larger than the increment due to changing the aspect ratio. The maximum lift coefficients decreased with increasing aspect ratio, mainly because of the associated increase in root thickness-chord ratio.

INTRODUCTION

Elementary aerodynamic considerations indicate that wings of high aspect ratio are essential for efficient long-range airplanes. Structural considerations for such wings favor relatively thick root sections and high taper ratios. Sections with large thickness-chord ratios have high profile drags, and high taper ratios usually result in impaired stalling characteristics. The aerodynamic advantages of high aspect ratio are thus partly offset by a design necessary to satisfy the structural requirements. Although the main aerodynamic effects of the design variables are readily calculated by lifting-line theory from section characteristics, considerable doubts have at times been expressed as to the absolute accuracy of the theory for determining an optimum combination of aspect ratio, taper ratio, and root thickness-chord ratio.

An investigation has accordingly been made in order (1) to demonstrate the correlation of wing characteristics obtained by calculation and by wind-tunnel tests and (2) to show some of the effects of aspect ratio, taper ratio, and root thickness-chord ratio on aerodynamic characteristics. Seven unswept wings having NACA 44-series sections, aspect ratios of 8, 10, and 12, and taper ratios of 2.5 and 3.5 were studied. For six of the wings, the ratio of span to root thickness was held constant at 35 so that the root thickness-chord ratio increased with increasing aspect ratio and decreased with increasing taper ratio. The seventh wing combined the lowest aspect ratio and taper ratio with the highest root thickness-chord ratio of the other wings. The wing characteristics were calculated by an application of the lifting-line theory which allows the use of the nonlinear section lift curves as well as by the usual application of the theory which assumes linear lift curves.

SYMBOLS

C_L lift coefficient (L/qS)

c_l	section lift coefficient (l/qc)
C_D	drag coefficient (D/qS)
C_{D_o}	profile-drag coefficient (D_o/qS)
C_m	pitching-moment coefficient (M'/qSc')
R	Reynolds number $(\rho V c'/\mu)$
M	Mach number (V/a)
q	free-stream dynamic pressure $\left(\frac{1}{2}\rho V^2\right)$
ρ	mass density of air
V	velocity of air in free stream
L	lift
l	section lift
D	total drag of wing
D_o	profile drag
M'	pitching moment about quarter-chord line
S	wing area
c'	mean aerodynamic chord $\left(\frac{2}{S}\int_0^{b/2} c^2\,dy\right)$
c	local chord
y	distance from plane of symmetry
b	wing span
μ	coefficient of viscosity
a	velocity of sound
α	angle of attack of wing root chord, degrees

c_s root chord

c_t construction tip chord

ϵ_t twist at construction tip

Subscripts:

min minimum

max maximum

(L = 0) at zero lift

WINGS

Seven wings of NACA 44-series sections with aspect ratios of 8, 10, and 12 and taper ratios of 2.5 and 3.5 were investigated. The wings had straight tapered plan forms with parabolic tips extending over the outer 5 percent of the semispan. There was neither dihedral nor sweep; that is, the quarter-chord line was perpendicular to the plane of symmetry. A typical wing layout is shown in figure 1.

Six of the wings were constructed to have a ratio of span to root thickness of 35 with the root thickness-chord ratio varying between 0.147 and 0.24; the seventh wing had a ratio of span to root thickness of 23.3 with a root thickness-chord ratio of 0.24. The tip thickness-chord ratio was 0.12 for all wings. Dimensional data for the wings are summarized in table I. The designation for the wings is formed from numbers representing, consecutively, the taper ratio, aspect ratio, NACA airfoil series, and root thickness in percent chord. For example, in the designation 2.5-8-44,16, the first number "2.5" represents the taper ratio, the number following the first dash "8" represents the aspect ratio (approx.), the number following the second dash "44" represents the NACA airfoil series, and the final number "16" represents the root thickness in percent chord.

The wings were twisted to improve the stalling characteristics. For the wings of taper ratio 2.5, twist was introduced to give a c_l-margin of approximately 0.1 at the 0.7 semispan station when $c_{l_{max}}$ was reached at some inboard wing section. (See references 1 and 2.) For the wings of taper ratio 3.5, calculations indicated that the washout necessary to provide this c_l-margin would cause excessive induced drag. The twist was therefore limited to 3° for this group of wings.

The wings were constructed of laminated mahogany and were finished with lacquer. Two surface conditions were provided for testing. For the smooth-model condition, the wings were sanded to an aerodynamically smooth finish. In order to simulate a rough-model condition, a leading-edge roughness similar to that established by the Langley two-dimensional low-turbulence pressure tunnel was used. The roughness was obtained by application of No. 60 (0.011-inch diameter) carborundum grains to a thin layer of shellac along the complete span over a surface length of 8 percent chord measured from the leading edge on both upper and lower surfaces. The grains were intended to cover 5 to 10 percent of the affected area. Some difficulty was encountered, however, in obtaining the same density of the grains for all wings. The roughness on the 2.5-8-44,24 wing was lighter than on the other wings and the aerodynamic characteristics of this wing are believed to be somewhat better than would be obtained with the desired roughness.

METHODS

Tests

The tests were conducted in the Langley 19-foot pressure tunnel with the wings mounted as shown in figure 2. For all tests the air in the tunnel was compressed to a density of approximately 0.0055 slug per cubic foot. The tests were made at several values of Reynolds number between 1.5×10^6 and 7.0×10^6. The Mach number range was from 0.06 to 0.25. The relation of Mach number to Reynolds number is given in figure 3. The relation of Mach number to Reynolds number varied from wing to wing because the change in aspect ratio was accomplished by changing the chord while the span constant was held constant.

Measurements of lift, drag, and pitching moment were made over an angle-of-attack range from -4° through the angle of stall. Profile-drag measurements were made by wake surveys at 24 spanwise stations at several angles of attack covering a lift-coefficient range from 0 to 1.0. Flow separation on the smooth wings was studied by means of wool tufts placed at 20, 40, 60, 80, and 90 percent of the chord and spaced 6 inches spanwise on the upper surface of the wing. No studies were made of the flow separation on the rough wing.

Corrections for support tare and interference have been applied to all force-test data. Jet-boundary and air-flow-misalinement corrections have been applied to the angle of attack and drag coefficient.

Calculations

The characteristics of the wings were calculated from two-dimensional airfoil data by the lifting-line theory. The required airfoil section characteristics at appropriate Reynolds numbers were obtained from unpublished data from the Langley two-dimensional low-turbulence pressure tunnel. These section data were obtained at a Mach number not exceeding 0.17, so that compressibility effects are believed to be negligible. The section data for the rough conditions were obtained for two sizes of carborundum grains so that the effect of the variation of relative grain size across the span of the tapered wings could be taken into account in the calculations for the wings with leading-edge roughness. Lift and induced drag characteristics were determined by a generalized application of the lifting-line theory which allows the use of nonlinear section lift curves and by the usual application which assumes linear lift curves. A correction to the lifting-line theory for the effect of chord of a finite-span wing was made by applying the edge-velocity factor given in reference 3. The profile-drag and pitching-moment coefficients were obtained by using section coefficients at the corresponding section lift coefficients and integrating the loadings across the span. The procedure by which the wing characteristics were computed is given in detail in reference 4. For the sake of brevity, the two applications of the theory mentioned previously are hereinafter referred to as the "generalized method" and the "linearized method".

Aerodynamic characteristics for the wings of taper ratio 2.5 were calculated by both the generalized and linearized methods for the smooth-model condition and by the generalized method for the rough-model condition. For the wings of taper ratio 3.5, the characteristics were calculated only for the smooth-model condition by the generalized method.

RESULTS AND DISCUSSION

Comparison of Experimental and Calculated Characteristics

The experimental and calculated lift, drag, and pitching-moment characteristics for the wings of taper ratio 2.5 and 3.5 are presented in figures 4 to 10 for the smooth-model condition. The experimental and calculated lift and drag characteristics for the wings of taper ratio 2.5 are given in figures 11 to 14 for the rough-model condition. Some of the important results of the comparisons are summarized in

tables II and III. For better accuracy, the experimental values of maximum lift-drag ratio $(L/D)_{max}$ given in these tables were read from faired curves of $(L/D)_{max}$ against Reynolds number.

Typical calculated spanwise distributions of section lift coefficients at the predicted maximum lift, for estimating stall characteristics, are given in figure 15. Experimental stall characteristics derived from tuft studies are shown in figures 16 and 17 for all smooth wings.

In the linear lift-curve range, the characteristics calculated by either the generalized or the linearized method would be expected to be the same. Differences in lift-curve slope and induced-drag coefficients were obtained, however, and are attributed to inaccuracies in computing that arose in reading, fairing, and integrating plotted curves.

Drag.- A comparison of the calculated and experimental total-drag curves for the smooth wings (figs. 4 to 10) shows that good agreement was obtained at low lift coefficients. Less satisfactory agreement was obtained at higher lift coefficients where the calculated drag was generally lower than the experimental drag. This effect was most pronounced for wings of aspect ratio 8. As would be expected, the same results are shown in a comparison of the calculated and experimental profile-drag coefficients. (Force-test profile-drag coefficients were determined by subtracting the induced drag coefficients obtained by calculation from the total drag coefficients measured by force tests.) The test values determined by wake surveys, however, are in excellent agreement with the calculated values. Possible reasons for discrepancy between force-test profile drag and calculated and wake-survey drag are (1) errors in corrections for support tare, interference, and stream misalinement, (2) inaccuracies in calculating induced drag and (3) inaccuracies in evaluating the drag at the wing tip from section data or wake surveys.

Generally speaking, the agreement between calculated and experimental drag for the rough condition (figs. 11 to 14) was about the same as for the smooth condition but was less consistent. In addition to the sources of errors mentioned before, errors in profile drag for the rough condition can easily arise from (1) inaccurate simulation of desired roughness in the wing tests and (2) inaccuracies in accounting for grain size in the calculations. These errors would also influence the lift characteristics.

For wings of the type investigated, the value of $(L/D)_{max}$ is a predominant factor in determining the optimum design. As indicated in tables II and III, the calculated values of $(L/D)_{max}$ were, for the case giving the greatest descrepancy, within 7 percent of the experimental

values. From the preceding discussion of possible errors in the determination of drag, even this largest difference between calculated and experimental $(L/D)_{max}$ appears reasonable.

Lift.- The differences between the values of maximum lift coefficient $C_{L_{max}}$ obtained from tests and from calculation by the generalized method (tables II and III) ranged from 0.02 to 0.08 with an average difference of about 0.04. The calculated values were generally lower than the experimental values. The maximum lift coefficients calculated by the linearized method are from 0 to 0.14 lower than the corresponding test values with an average difference of about 0.07. The maximum lift coefficient calculated by the linearized method is the wing lift coefficient at which some section first reached maximum lift. The generalized method of calculation predicts the rounded lift curve peaks as were obtained by test in contrast to the straight curves predicted by the linearized method.

The agreement between experimental and calculated lift-curve slopes at low angles of attack (tables II and III) is not altogether satisfactory. The correlation is good for the wings of aspect ratio 8. For the other wings, the calculated values were as much as 4 percent lower than the experimental values in some cases. Aside from experimental and computing errors, discrepancies may be due to the limitations of the edge-velocity factor in correcting for the effect of the chord in three-dimensional flow. The agreement between experimental and calculated angles of zero lift is excellent.

Pitching moment.- At zero lift the agreement between the experimental and calculated pitching-moment coefficients and moment-curve slopes is generally good. (See table II.) At higher lifts, however, the experimental pitching-moment curves show larger increases in slope than the calculated curves. (See figs. 4 to 10.)

Stalling characteristics.- In order to obtain an indication of the stalling characteristics of the wings, an analysis of the type outlined in references 1 and 2 was made by comparing the predicted distribution of section lift coefficients at maximum lift with the variation of section maximum lift across the span. A comparison of this type for the 2.5-10-44,20 and 3.5-10-44,18.4 wings is shown in figure 15. On the basis of the curves calculated by the generalized method, the maximum section lift coefficients for these wings appear to be reached simultaneously over most of the span. The corresponding tuft surveys (figs. 16 and 17), which show trailing-edge separation or intermittent separation over approximately the same part of the span, are accordingly in general agreement with the calculations; however, a more quantitative discussion of the agreement is not

possible in the absence of an experimental span load distribution and a correlation between section lift coefficient and tuft behavior. The difference between the two calculated curves of figure 15(a) is sufficiently great to affect seriously any prediction of stalling characteristics. For this wing the generalized method predicts the maximum section lift coefficients to be reached simultaneously over most of the span, whereas the linearized method indicates a considerable margin of safety at the outboard sections when the inboard sections have reached maximum lift.

The comparison indicates that the criterion of a c_l-margin of 0.1 at the 0.7 semispan station, which appears to be satisfied on the basis of the linearized method, is not actually attained if it is to be assumed that the generalized method is more correct. If the margin of 0.1 is necessary for good lateral stability and control, the stalling characteristics of the wing would be unsatisfactory according to the generalized method. On the basis of the tuft surveys alone, the stalling of these wings might be considered satisfactory since it is gradual and characterized by initial roughness and separation near the center and by fair flow at maximum lift.

Remarks.- Although calculated force and moment characteristics show some variations with respect to the experimental characteristics, the agreement is reasonable and is believed to be close enough to warrant their use in design. For calculating characteristics at high lifts, the method based on nonlinear section lift curves was more accurate than the method based on linear lift curves. The results of the investigation indicate the need for more accurate methods for predicting flow separation on a wing.

Effects of Aspect Ratio, Taper Ratio, and Root Thickness-Chord Ratio

The experimental characteristics of the wings are compared in figures 18 and 19. Calculated profile-drag coefficients are presented in figure 20. The variations of $(L/D)_{max}$ with aspect ratio are shown in figure 21. The experimental variations of $C_{L_{max}}$ and $(L/D)_{max}$ with Reynolds number are given in figure 22. In the following discussion the wings are compared at an essentially constant value of Reynolds number of approximately 3.9×10^6. Although data included in table II and figure 18(a) are for a Reynolds number different from 3.9×10^6, the comparisons shown by these data are essentially the same as for a Reynolds number of 3.9×10^6.

Drag.- The drag curves for the smooth wings (fig. 18) show the characteristic decrease in drag with increase in aspect ratio at moderate lift coefficients even though the profile drag was increased by the thicker root sections of the higher-aspect-ratio wings. Similar variations were obtained in the rough condition for the wings of taper ratio 3.5 and for wings of taper ratio 2.5 with aspect ratios 8 and 10. (See fig. 19.) The wing of aspect ratio 12 and taper ratio 2.5 had higher drags, however, than the wing of aspect ratio 10 except near the C_L for $(L/D)_{max}$ where the drags of the two wings were equal. The calculated data in figure 20 indicate that this effect is associated with the relatively large profile drag of the thicker root sections of the high-aspect-ratio wings in the rough condition.

The same variations in drag with aspect ratio are shown by consideration of the values of $(L/D)_{max}$ in figure 21. For the wings of taper ratio 2.5, both experimental and calculated values of $(L/D)_{max}$ for the smooth condition increased with increasing aspect ratio throughout the range of aspect ratios investigated but the values for the rough condition indicated no gain in $(L/D)_{max}$ when the aspect ratio is increased from 10 to 12. For the wings of taper ratio 3.5, the values of $(L/D)_{max}$ for both the smooth and rough conditions increased with increasing aspect ratio. Figure 21 also indicates that the harmful effects of roughness on $(L/D)_{max}$ can readily exceed the beneficial effects of increasing aspect ratio in this range; it may be noted, however, that the roughness was somewhat extreme. Generally, there was little difference in $(L/D)_{max}$ for corresponding wings of taper ratio 2.5 and 3.5 in the smooth condition but in the rough condition the values of $(L/D)_{max}$ for the wings of taper ratio 3.5 were consistently higher than those for the wings of taper ratio 2.5. This difference was probably due to the larger effect of roughness on the thicker sections of the wings of 2.5 taper ratio. The data in figure 22 indicated that Reynolds number generally had little effect on the $(L/D)_{max}$ of the smooth wings and that increasing the Reynolds number increased the $(L/D)_{max}$ of the rough wings.

Lift.- For both smooth and rough conditions, the maximum lift coefficients of the wings with a ratio of span to root thickness of 35 decreased with increasing aspect ratio. An apparent decrease in $C_{L_{max}}$ due to aspect ratio alone is noted by a comparison of wings 2.5-8-44,24 and 2.5-12-44,24 (fig. 22) but this decrease was probably due to the fact that, when the two wings were at the same Reynolds number, the

wing of aspect ratio 12 was at the higher Mach number. The wings of taper ratio 3.5 had higher values of $C_{L_{max}}$ than did the wings of taper ratio 2.5 but the difference was usually negligible. The maximum lift coefficients increased with Reynolds number over most of the range. At the upper end of the range, the value of $C_{L_{max}}$ for some of the wings decreased, probably because of compressibility effects.

The lift-curve slope $dC_L/d\alpha$ for the smooth wings shows the characteristic increase with increasing aspect ratio (table II). For the rough wings (table III), the lift curves show little change in slope as a result of the large adverse effects of section thickness ratio.

Stall characteristics.- The results of the stall studies in figures 16 and 17 show that all the wings have similar stall patterns. Separation of flow began at the trailing edge near the root and gradually progressed forward and outward until, at $C_{L_{max}}$, 30 to 40 percent of the wing was stalled. The effects on stall characteristics of increasing the taper ratio from 2.5 to 3.5 were very small.

CONCLUSIONS

The aerodynamic characteristics of seven unswept tapered wings were determined by calculation from two-dimensional data and by wind-tunnel tests in order to demonstrate the accuracy of the calculations and to show some of the effects of aspect ratio, taper ratio, and root thickness-chord ratio. On the basis of comparisons made at equal values of Reynolds number, the following conclusions are shown:

1. Reasonable agreement was obtained between calculated and experimental wing force and moment characteristics. The method of calculation which allowed the use of nonlinear section lift curves gave better agreement with experiment at high angles of attack than did the method which assumed linear lift curves. The two methods of calculation gave different spanwise lift distributions at maximum lift.

2. The values of maximum lift-drag ratio $(L/D)_{max}$ of the smooth wings increased with increasing aspect ratio throughout the range investigated in spite of the increased drag of the thicker root sections associated with the higher aspect ratios. The values of $(L/D)_{max}$

for the rough wings of taper ratio 3.5 indicated the same trend; however, the values for the wings of taper ratio 2.5 showed no gain when the aspect ratio was increased from 10 to 12, apparently because of the larger increment of profile drag due to roughness on the thicker root sections of the wing of aspect ratio 12. The decrement in $(L/D)_{max}$ due to roughness was considerably greater than the increment due to changing the aspect ratio through the entire range investigated.

3. The maximum lift coefficients decreased with increasing aspect ratio mainly because of the associated increase in root thickness-chord ratio.

Langley Memorial Aeronautical Laboratory
National Advisory Committee for Aeronautics.
Langley Field, Va., November 25, 1946

REFERENCES

1. Anderson, Raymond F.: A Comparison of Several Tapered Wings Designed to Avoid Tip Stalling. NACA TN No. 713, 1939.

2. Soulé, H. A., and Anderson, Raymond F.: Design Charts Relating to the Stalling of Tapered Wings. NACA Rep. No. 703, 1940.

3. Jones, Robert T.: Correction of the Lifting-Line Theory for the Effect of the Chord. NACA TN No. 817, 1941.

4. Sivells, James C., and Neely, Robert H.: Method for Calculating Wing Characteristics by Lifting-Line Theory Using Nonlinear Section Lift Data. NACA TN No. 1269, 1947.

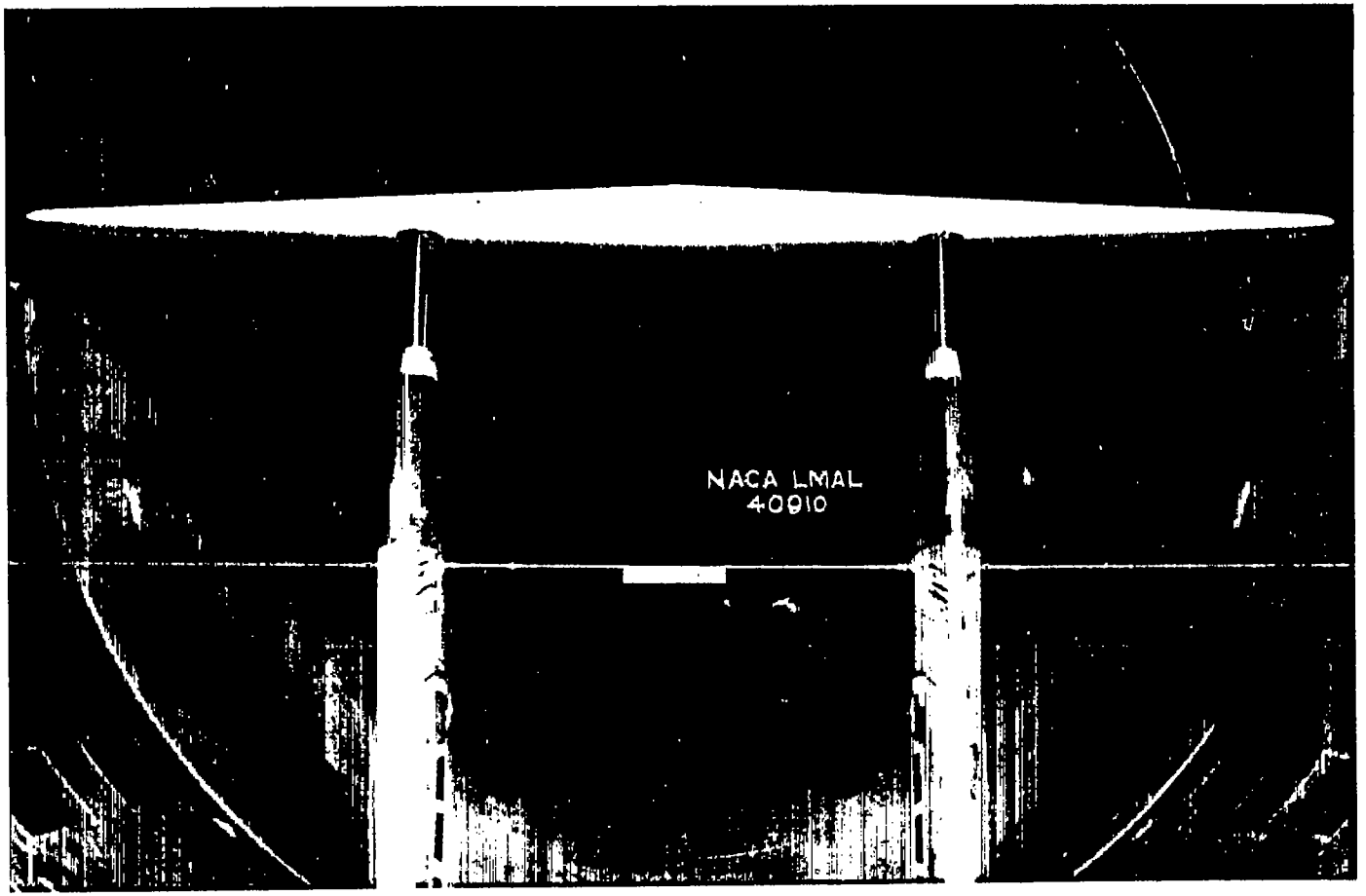

Figure 2.- Wing mounted in Langley 19-foot pressure tunnel.

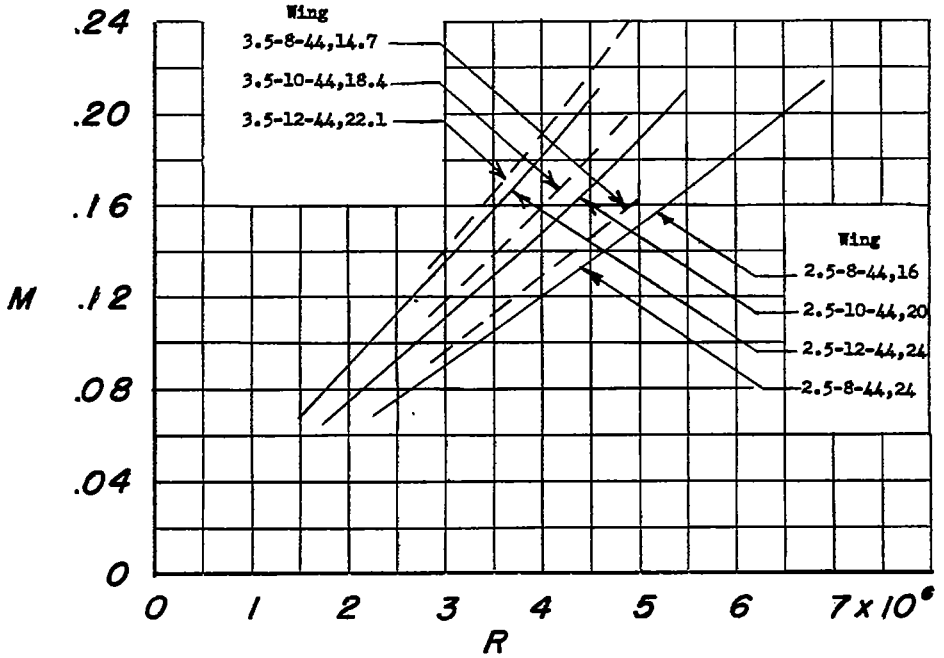

(a) Smooth leading edge.

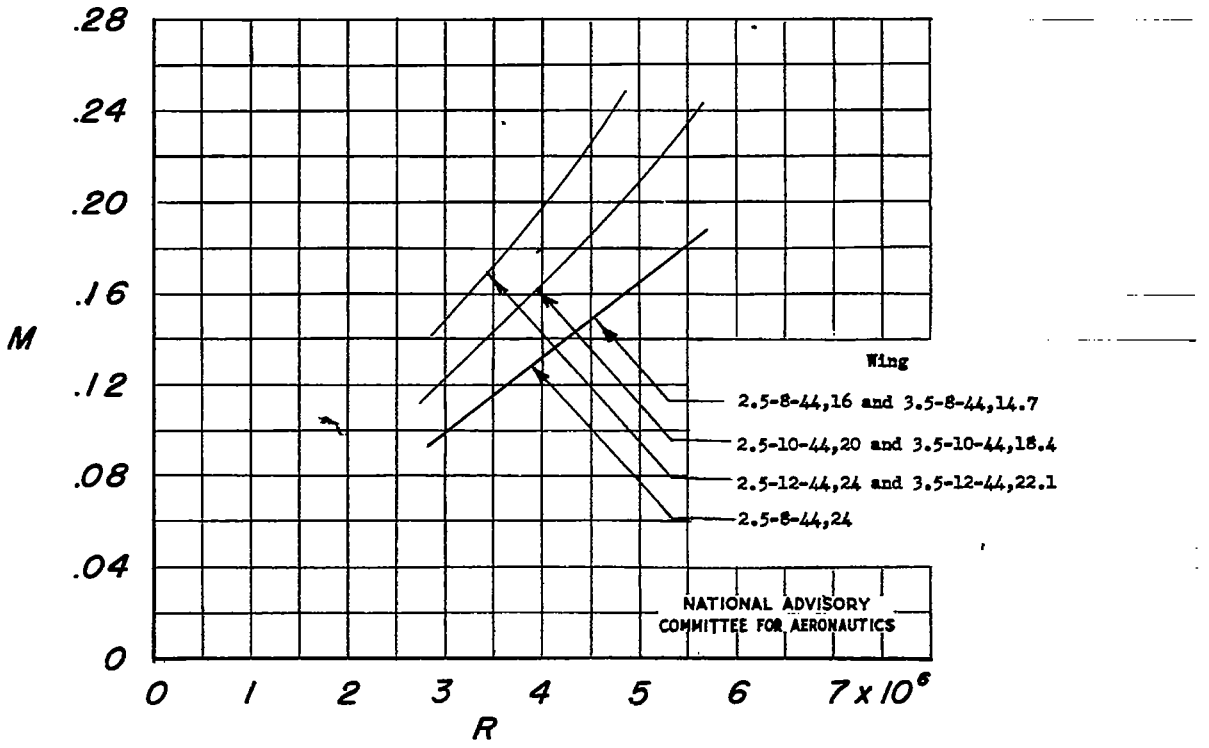

(b) Rough leading edge.

Figure 3.- Relation of experimental Mach number to Reynolds number.

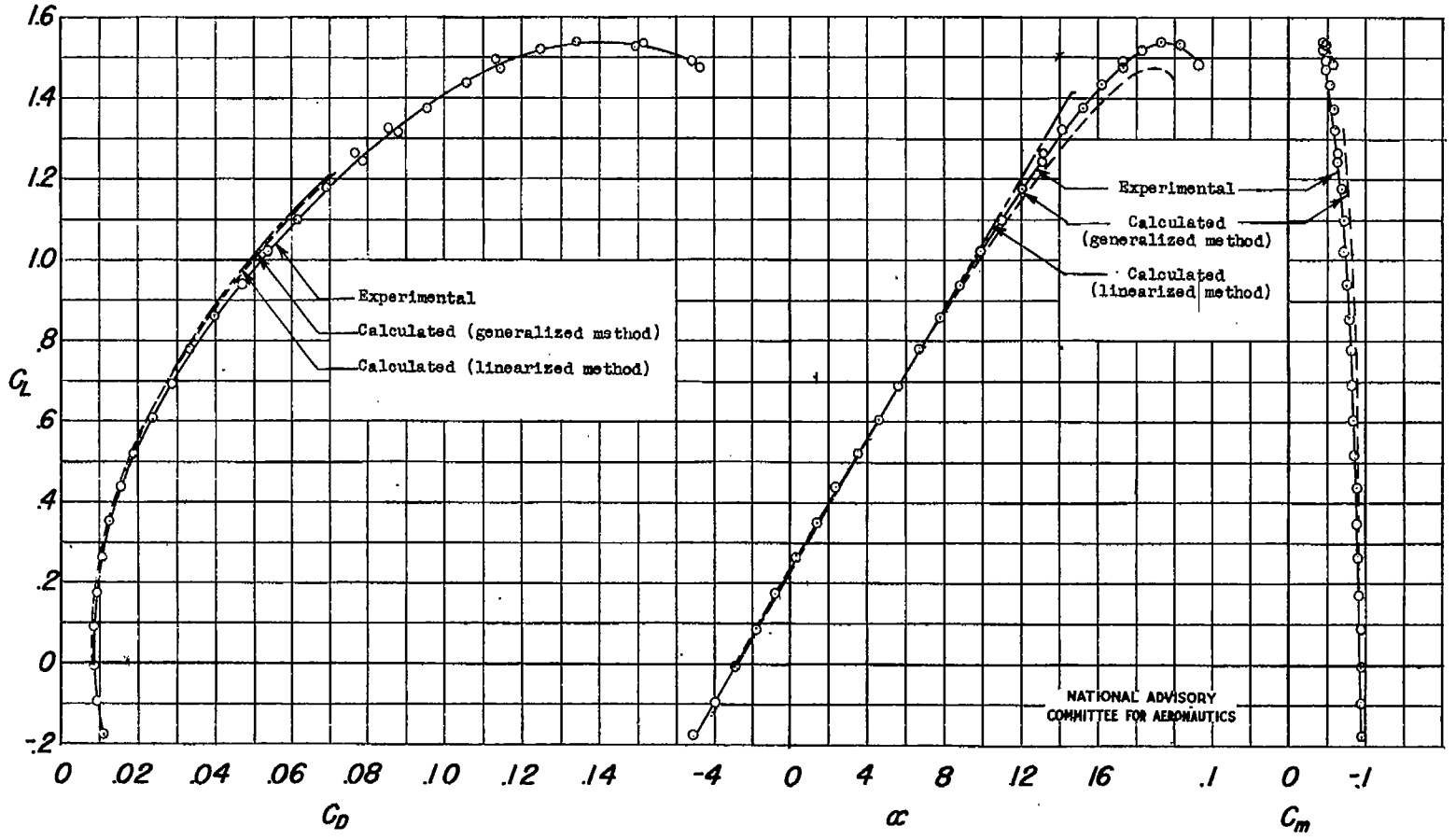

(a) C_L against C_D, α, and C_m.

Figure 4.- Experimental and calculated characteristics of wing 2.5-8-44,16 with smooth leading edge. $R = 4.32 \times 10^6$.

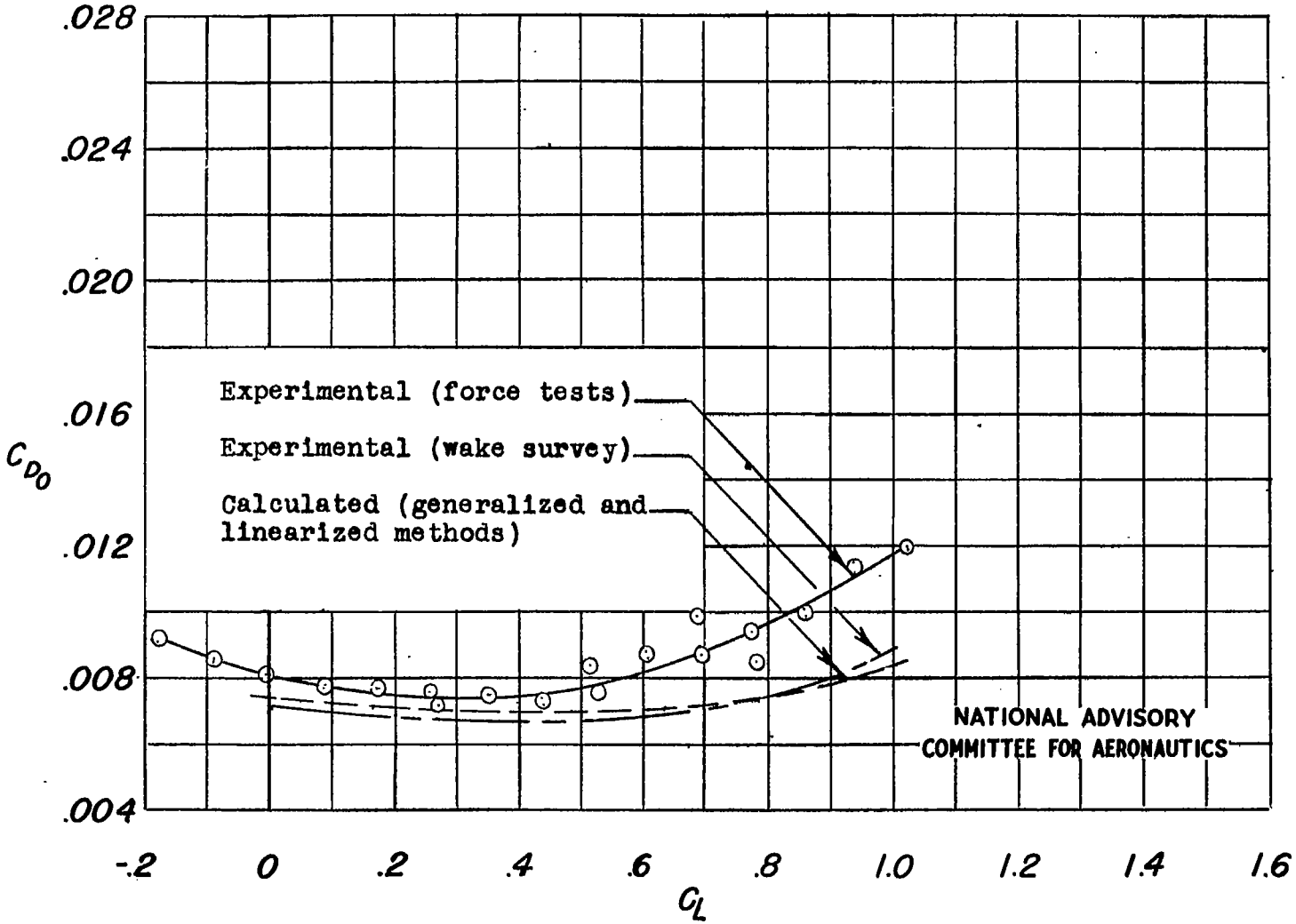

(b) C_{D_o} against C_L.

Figure 4.- Concluded.

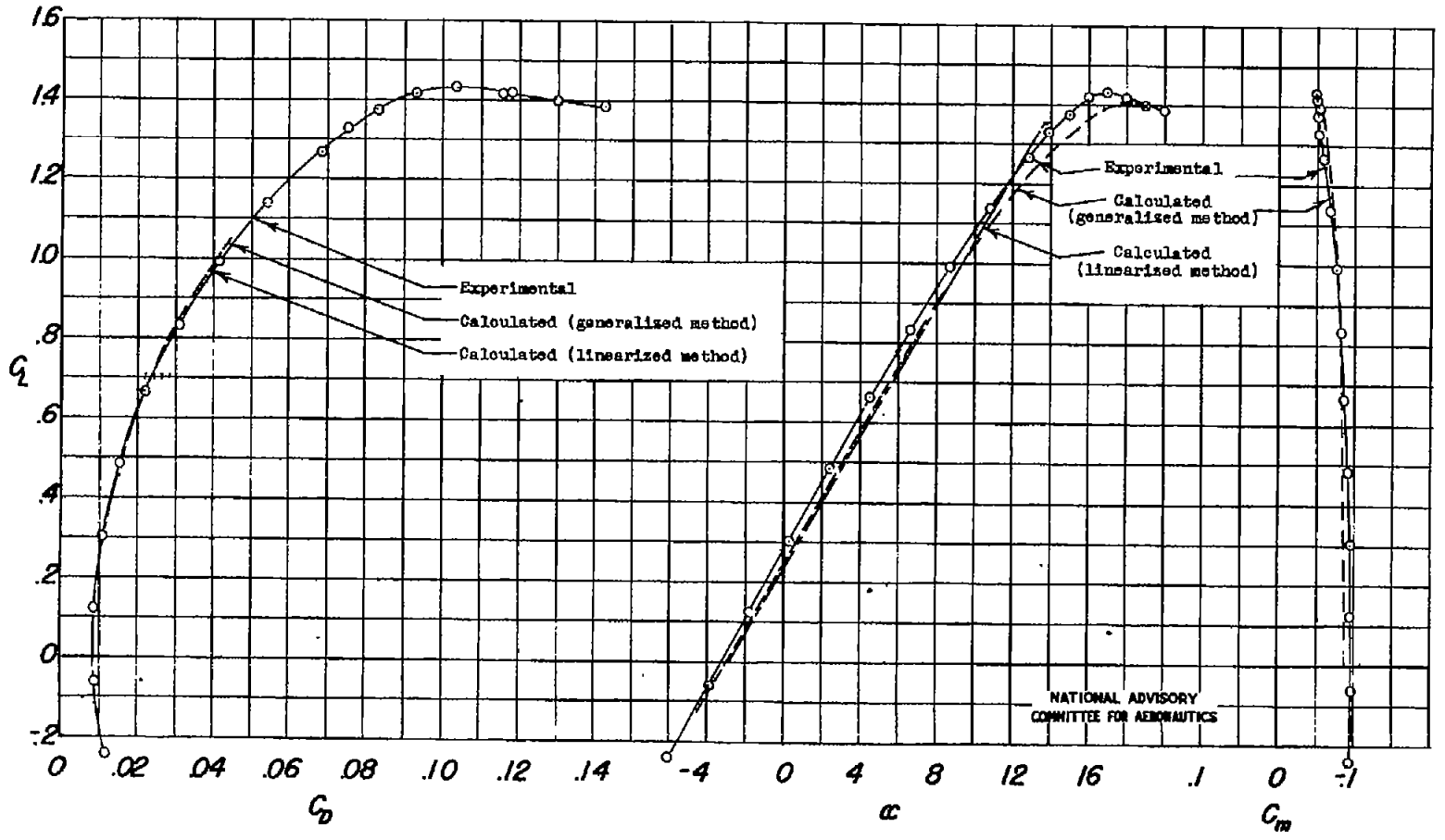

(a) C_L against C_D, α, and C_m.

Figure 5.- Experimental and calculated characteristics of wing 2.5-10-44,20 with smooth leading edge. $R = 3.49 \times 10^6$.

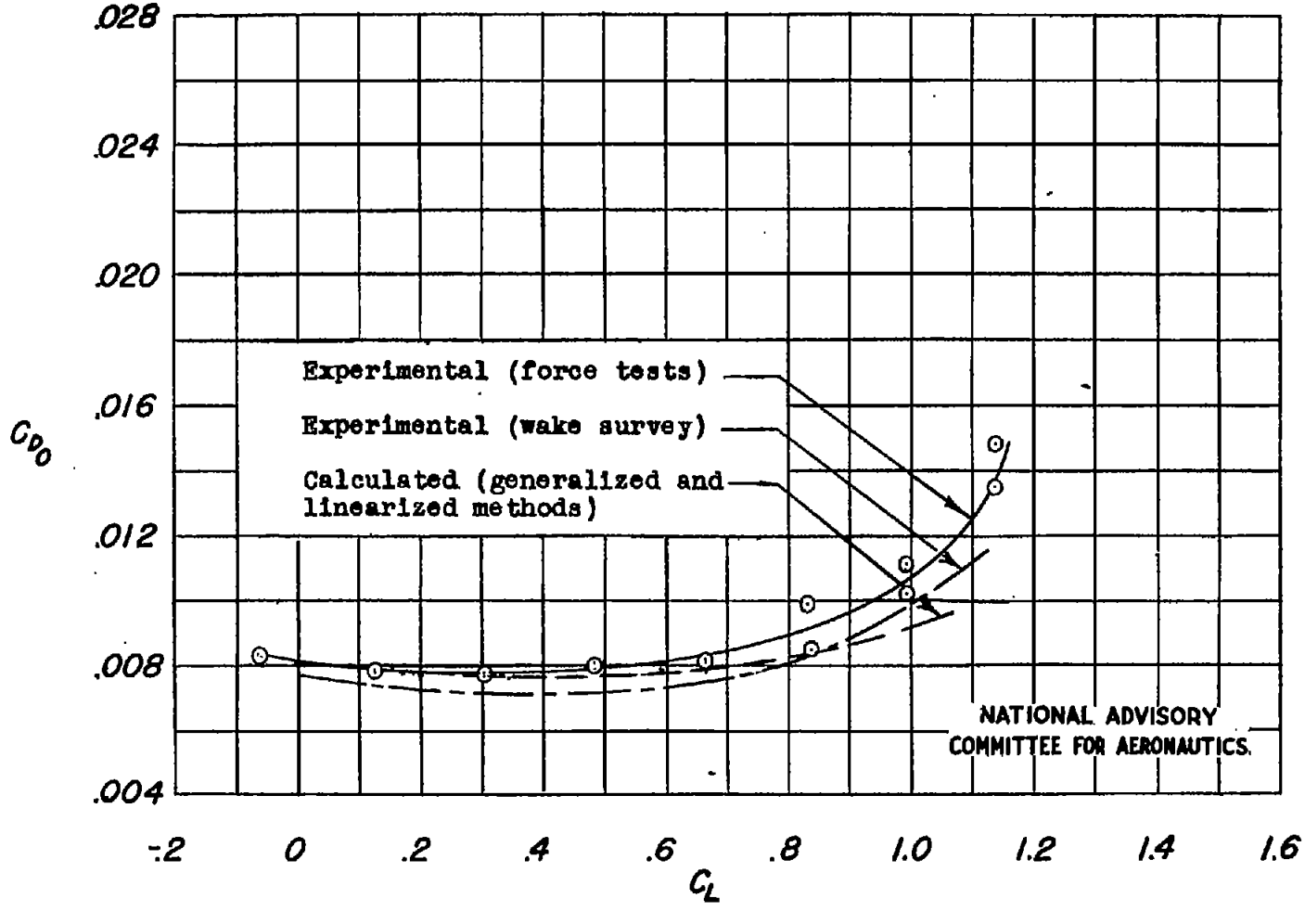

(b) C_{D_o} against C_L.

Figure 5.- Concluded.

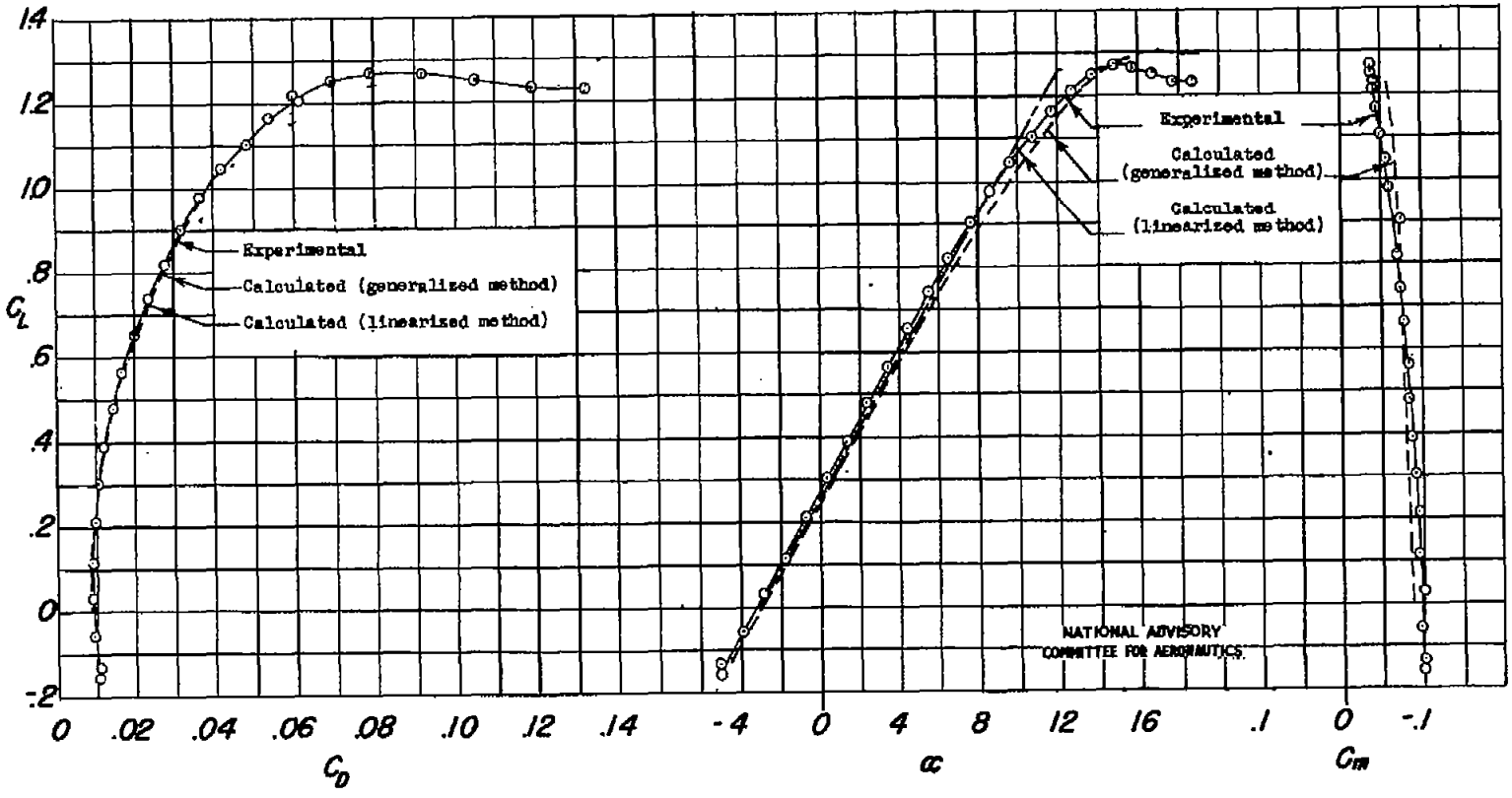

(a) C_L against C_D, α, and C_m.

Figure 6.- Experimental and calculated characteristics of wing 2.5-12-44,24 with smooth leading edge. $R = 2.87 \times 10^6$.

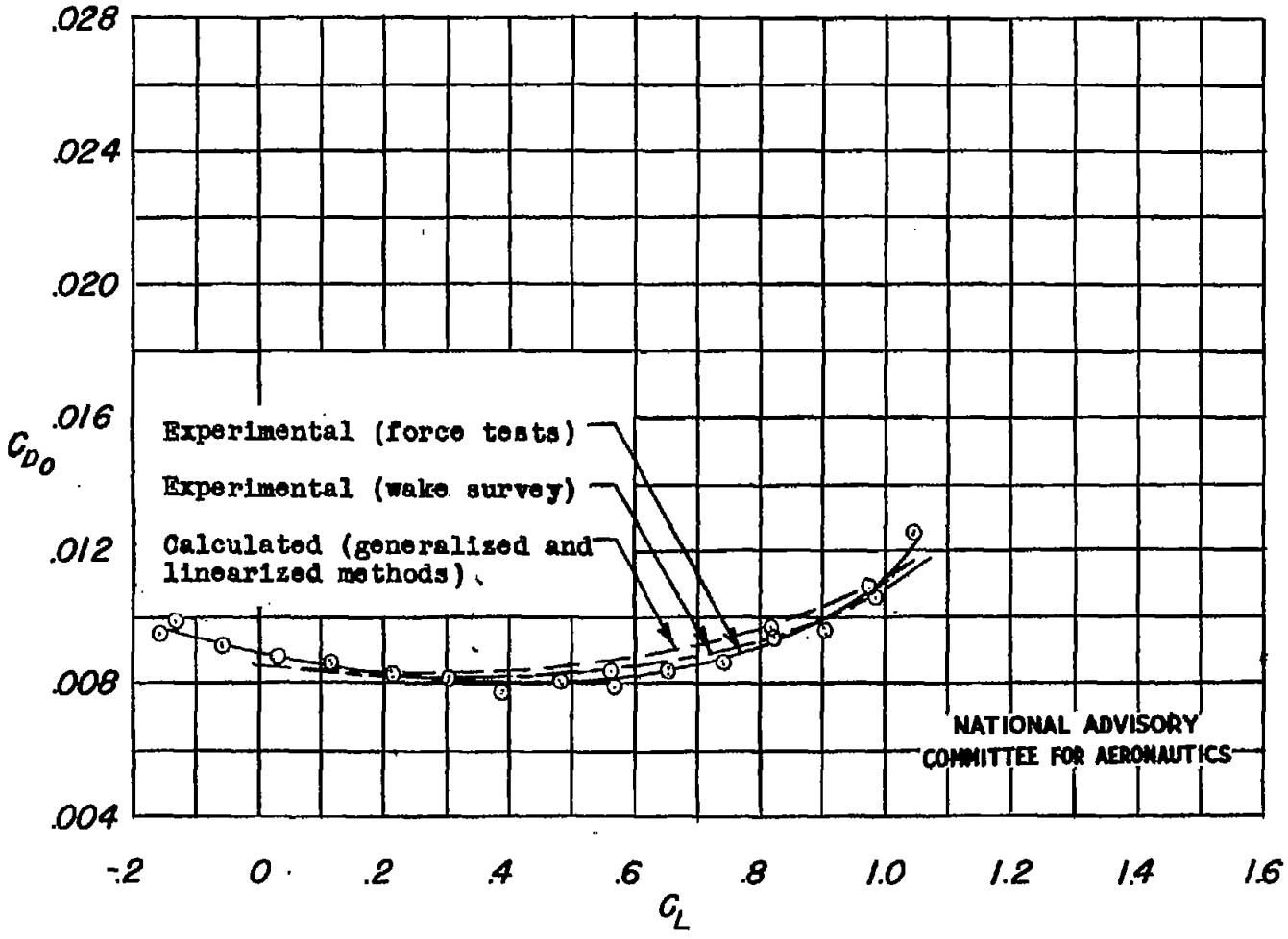

(b) C_{D_o} against C_L.

Figure 6.- Concluded.

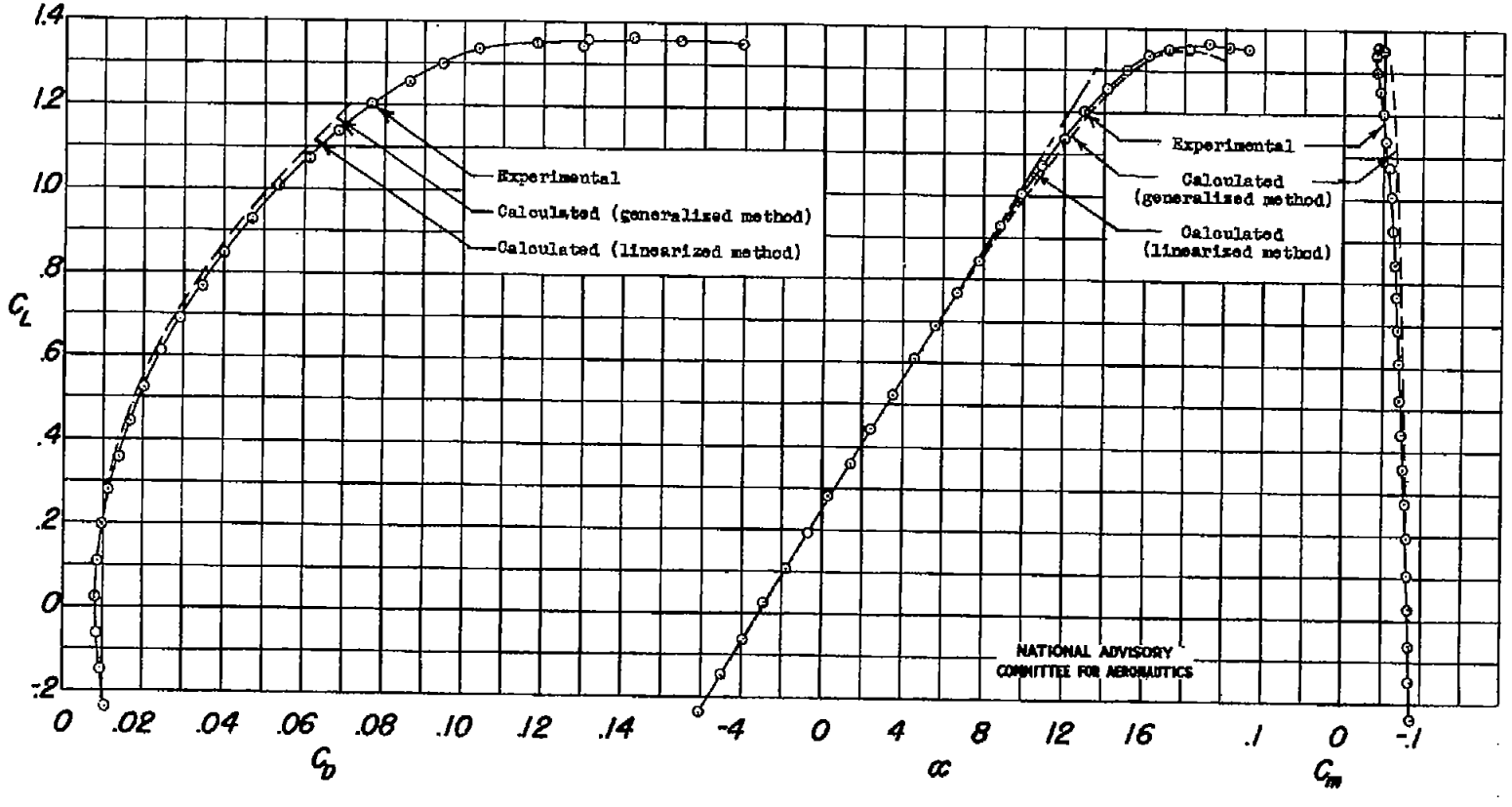

(a) C_L against C_D, α, and C_m.

Figure 7.- Experimental and calculated characteristics of wing 2.5-8-44,24 with smooth leading edge. $R = 4.32 \times 10^6$.

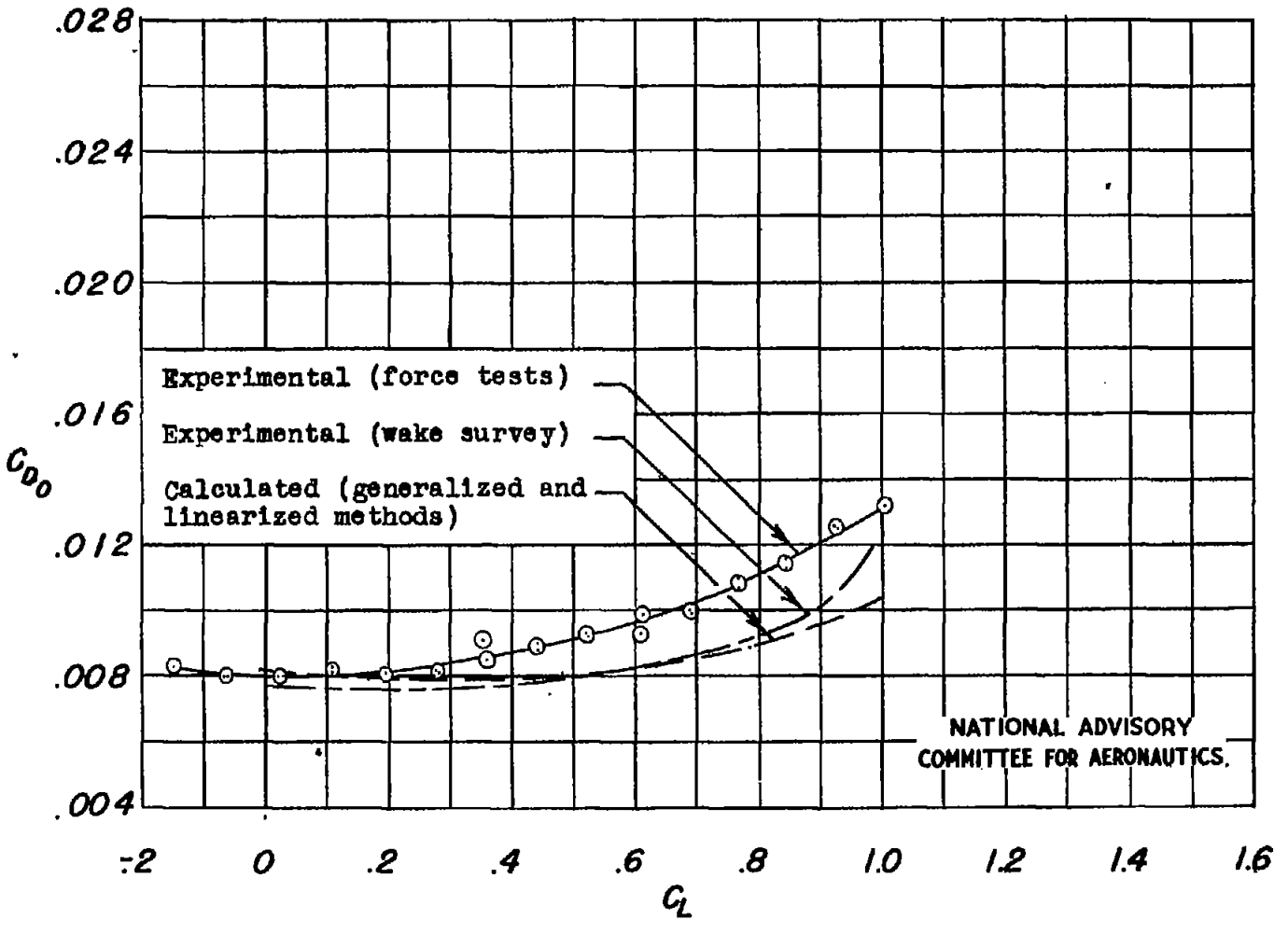

(b) C_{D_o} against C_L.

Figure 7.- Concluded.

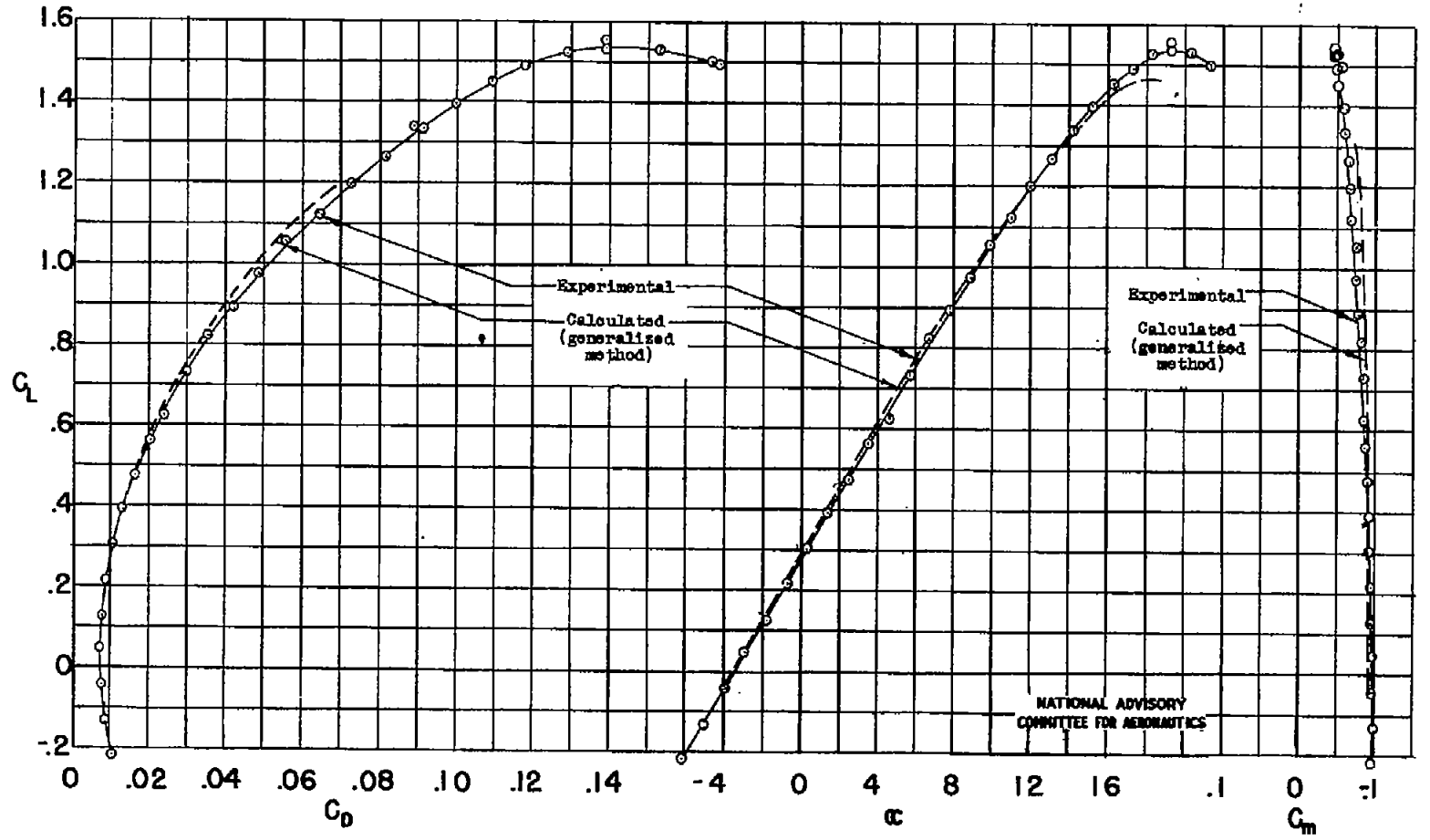

(a) C_L against C_D, α, and C_m.

Figure 8.- The experimental and calculated characteristics of wing 3.5-8-44,14.7 with smooth leading edge. $R = 4.0 \times 10^6$.

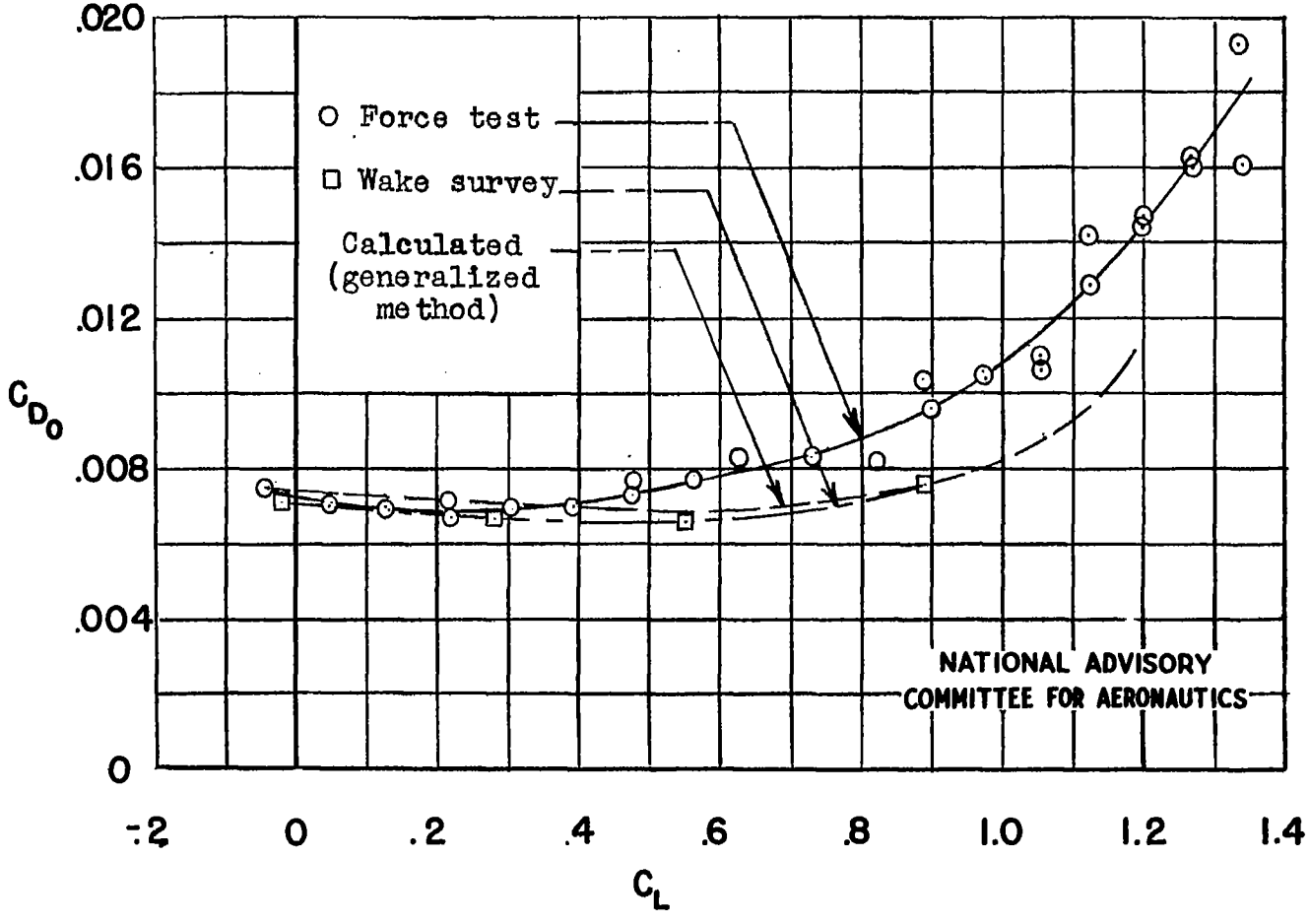

(b) C_{D_o} against C_L.

Figure 8.- Concluded.

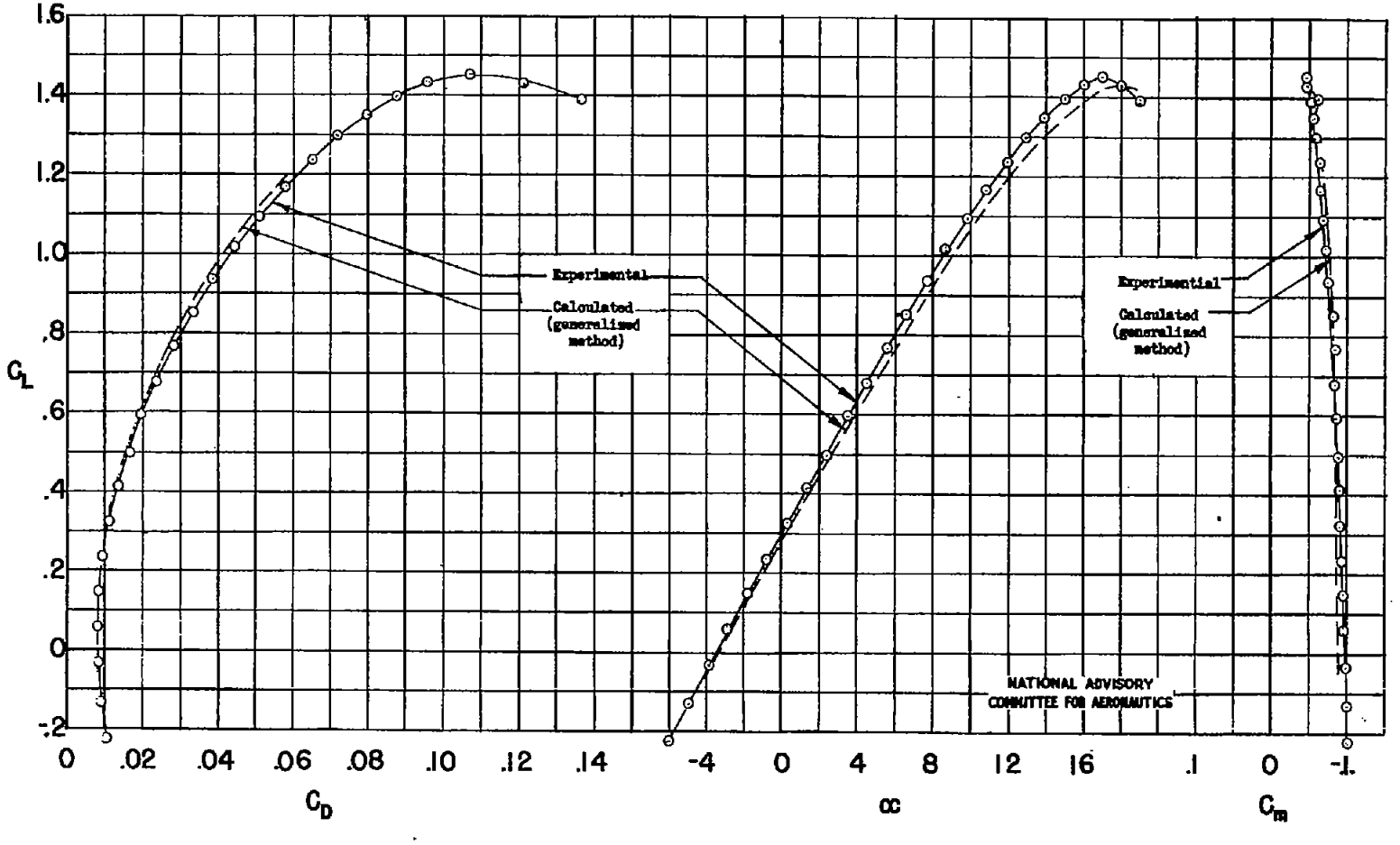

(a) C_L against C_D, α, and C_m.

Figure 9.- The experimental and calculated characteristics of wing 3.5-10-44,18.4 with smooth leading edge. $R = 4.0 \times 10^6$.

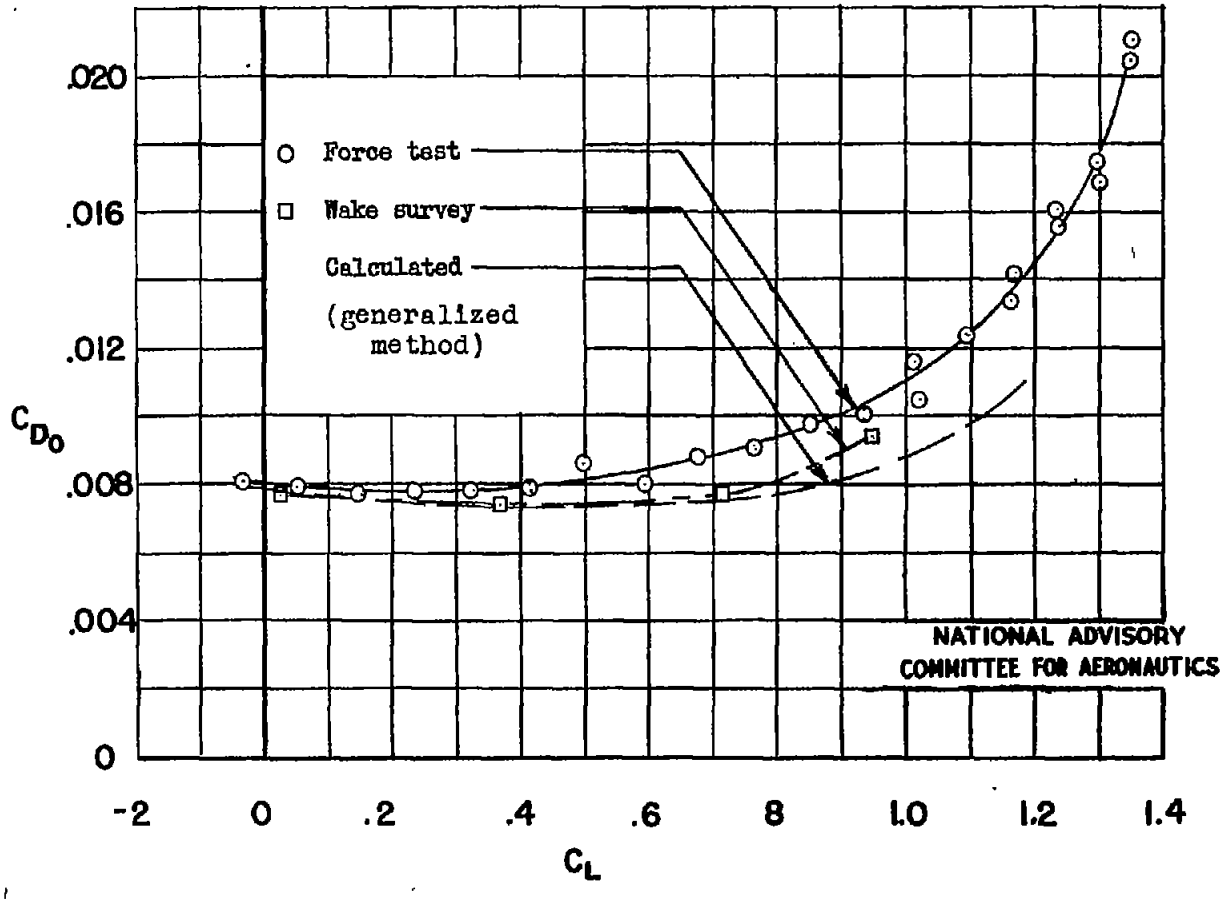

(b) C_{D_o} against C_L.

Figure 9.- Concluded.

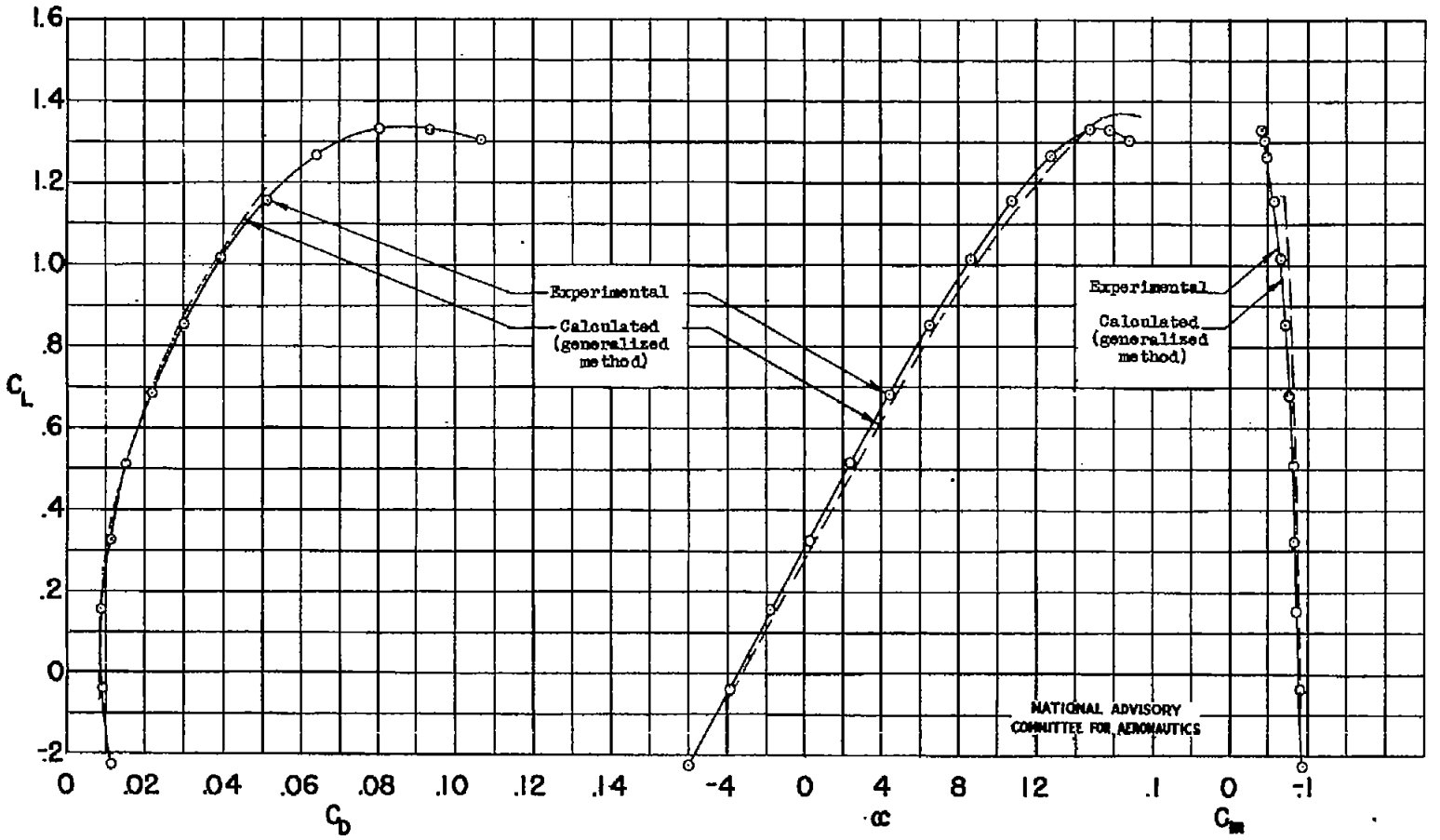

(a) C_L against C_D, α, and C_m.

Figure 10.- The experimental and calculated characteristics of wing 3.5-12-44,22.1 with smooth leading edge. $R = 4.0 \times 10^6$.

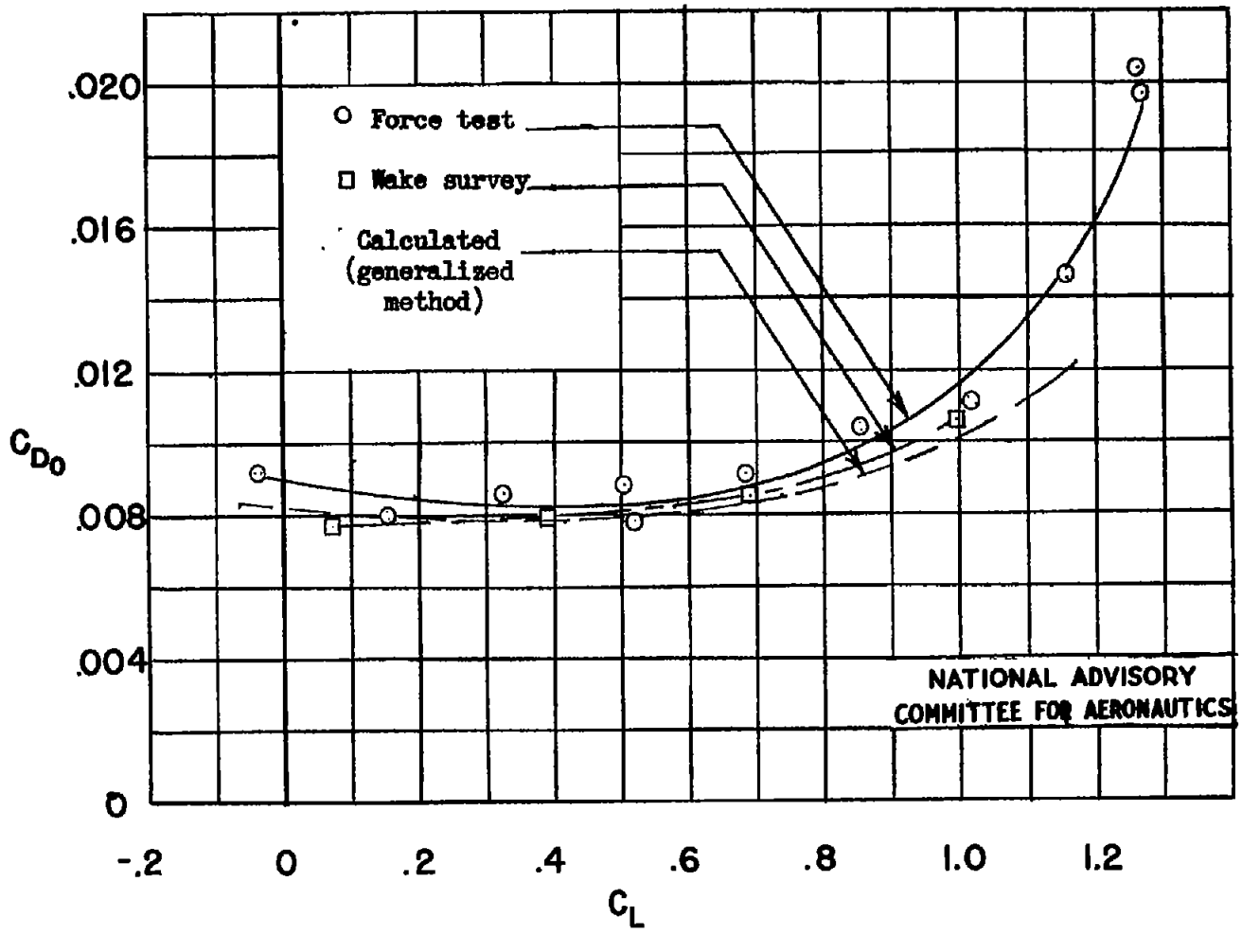

(b) C_{D_o} against C_L.

Figure 10.- Concluded.

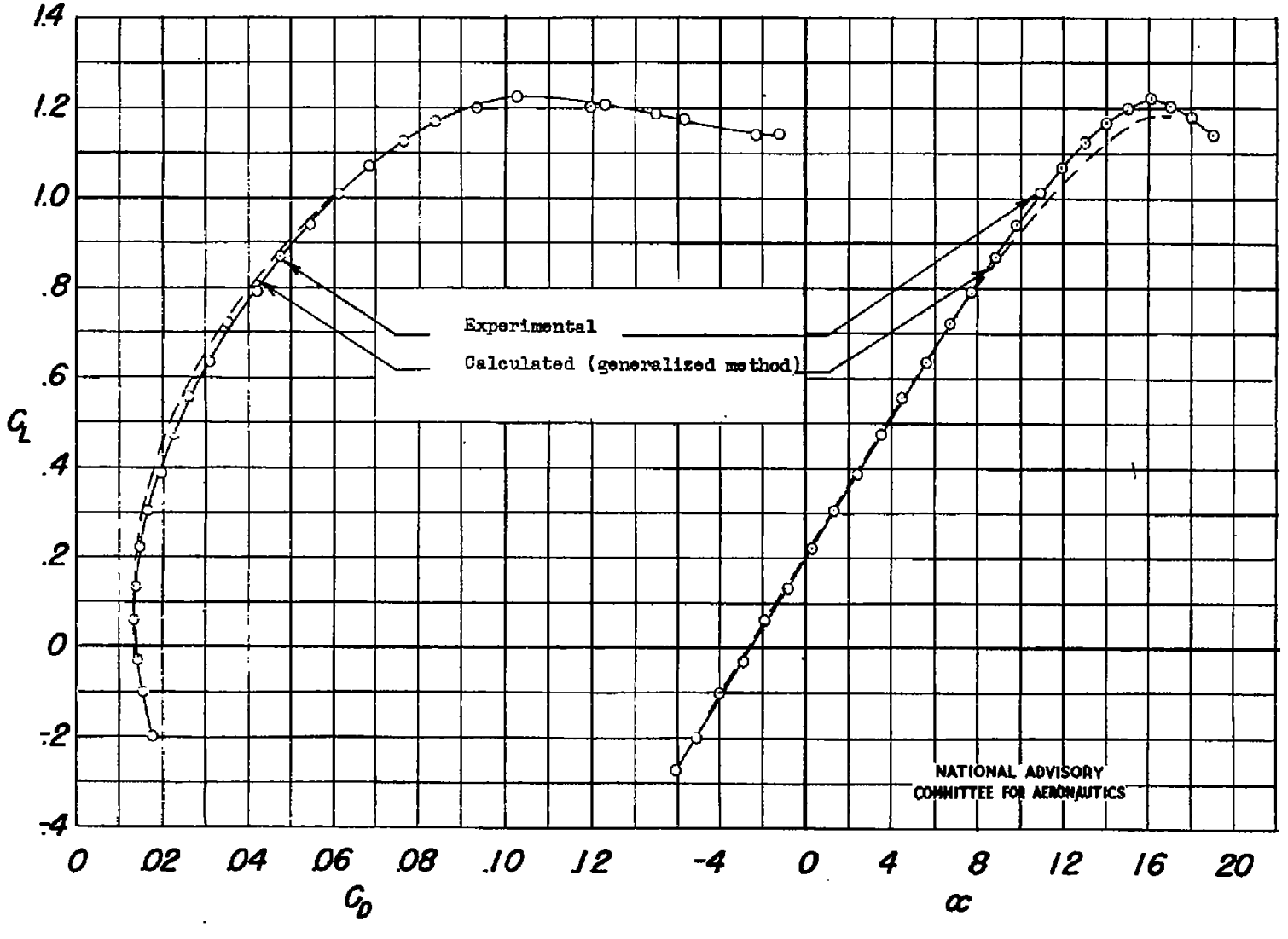

Figure 11.- Experimental and calculated characteristics of wing 2.5-8-44,16 with rough leading edge. $R = 3.9 \times 10^6$.

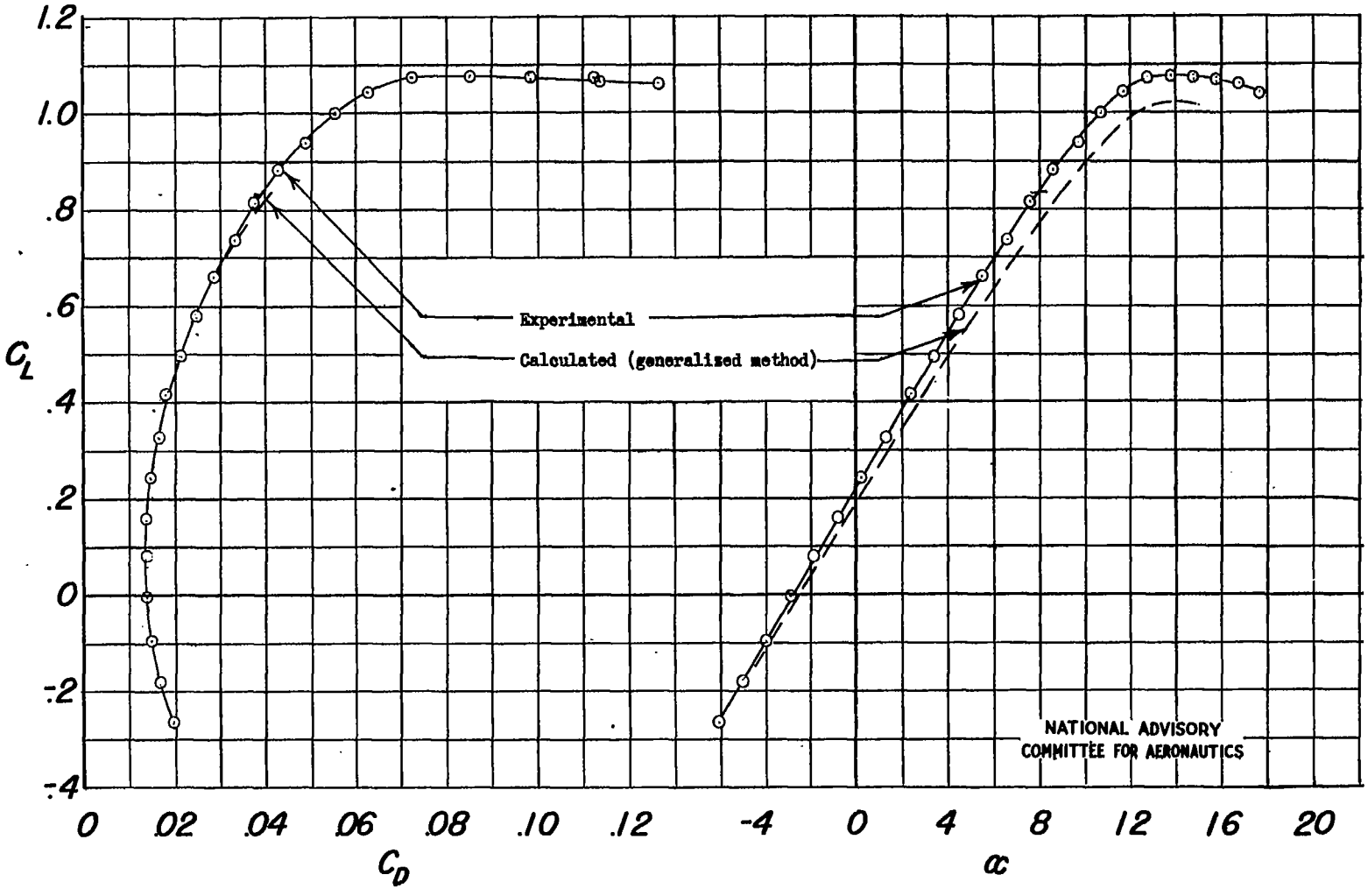

Figure 12.- Experimental and calculated characteristics of wing 2.5-10-44,20 with rough leading edge. $R = 3.9 \times 10^6$.

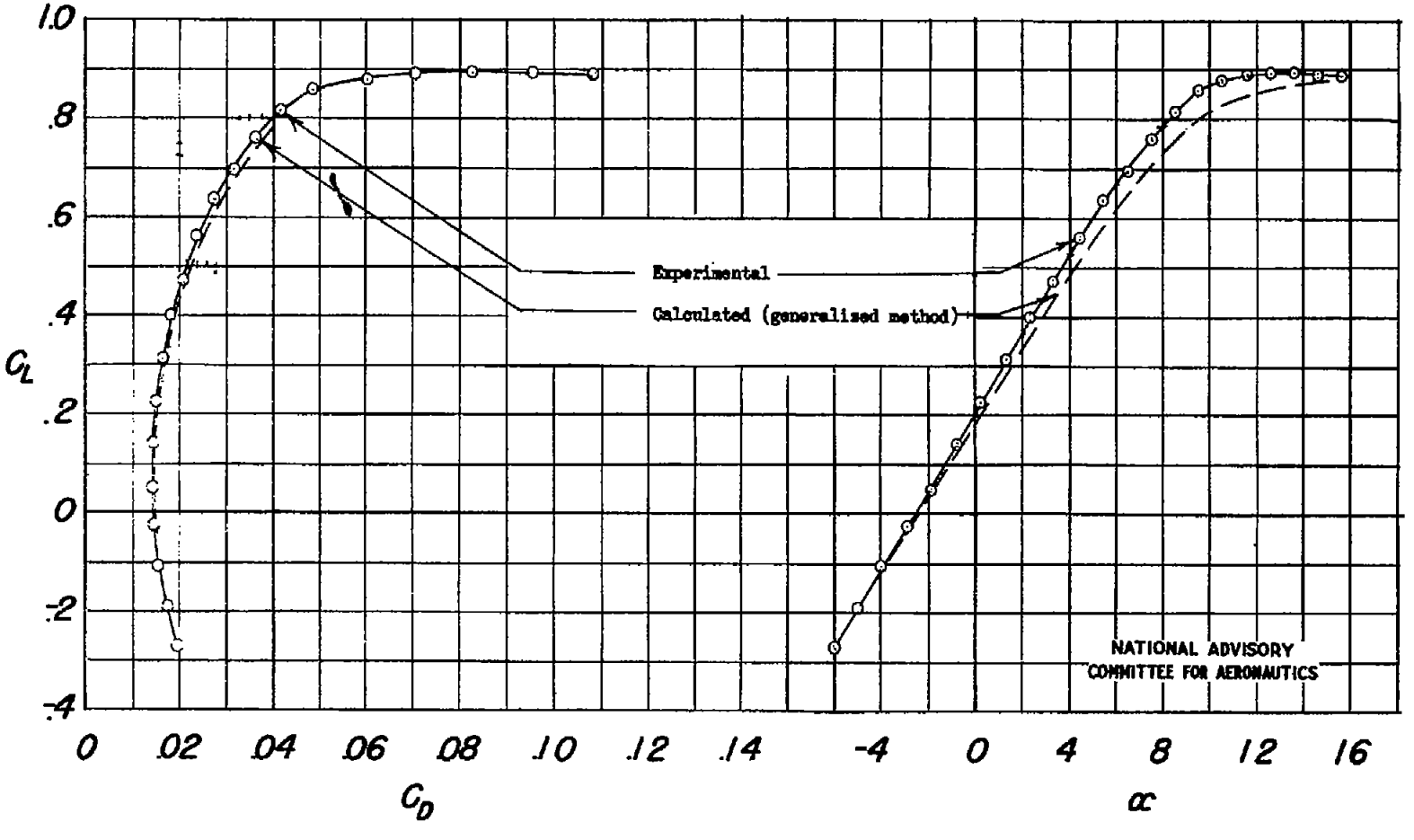

Figure 13.- Experimental and calculated characteristics of wing 2.5-12-44,24 with rough leading edge. $R = 3.9 \times 10^6$.

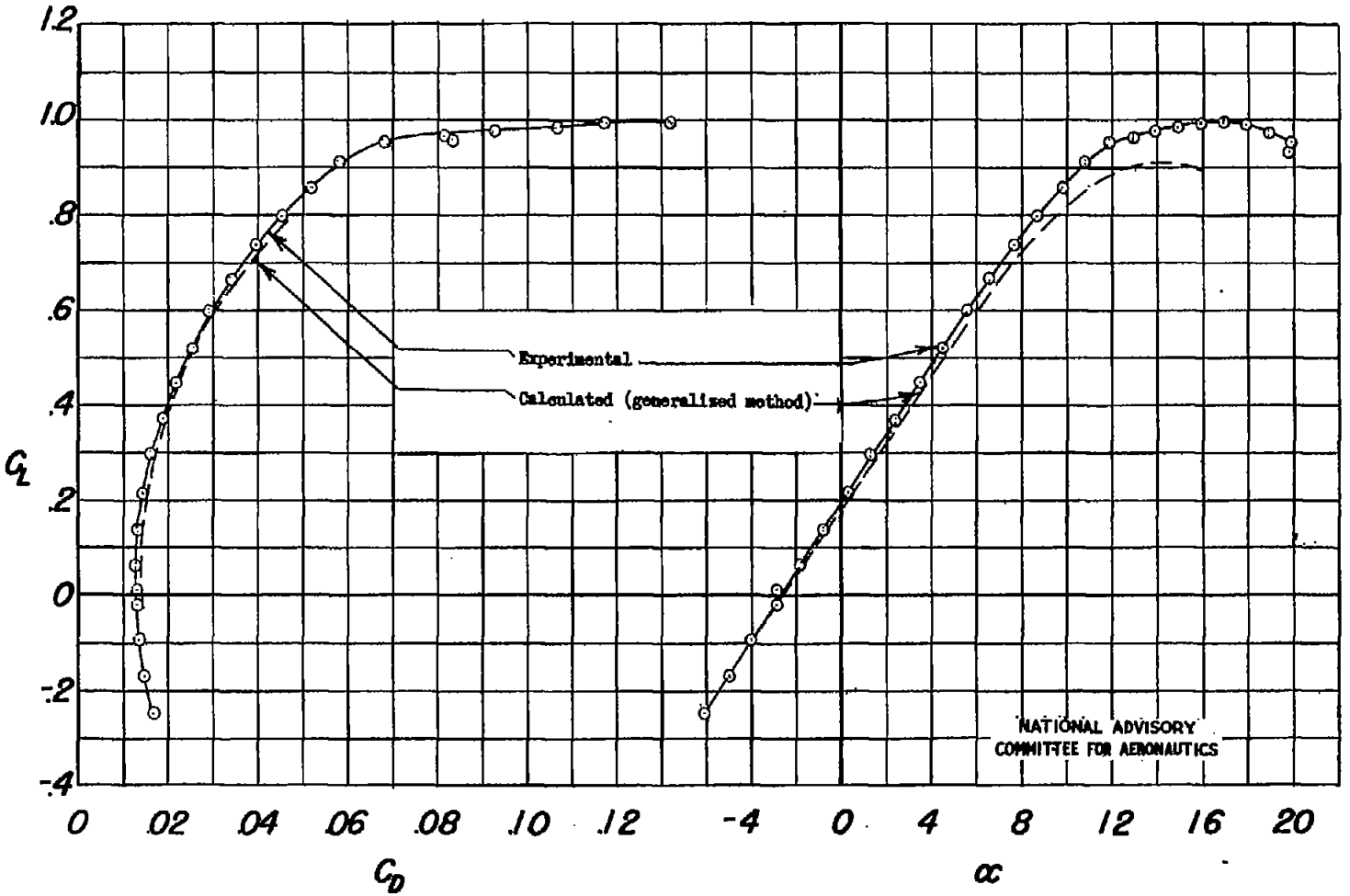

Figure 14.- Experimental and calculated characteristics of wing 2.5-8-44,24 with rough leading edge. $R = 3.9 \times 10^6$.

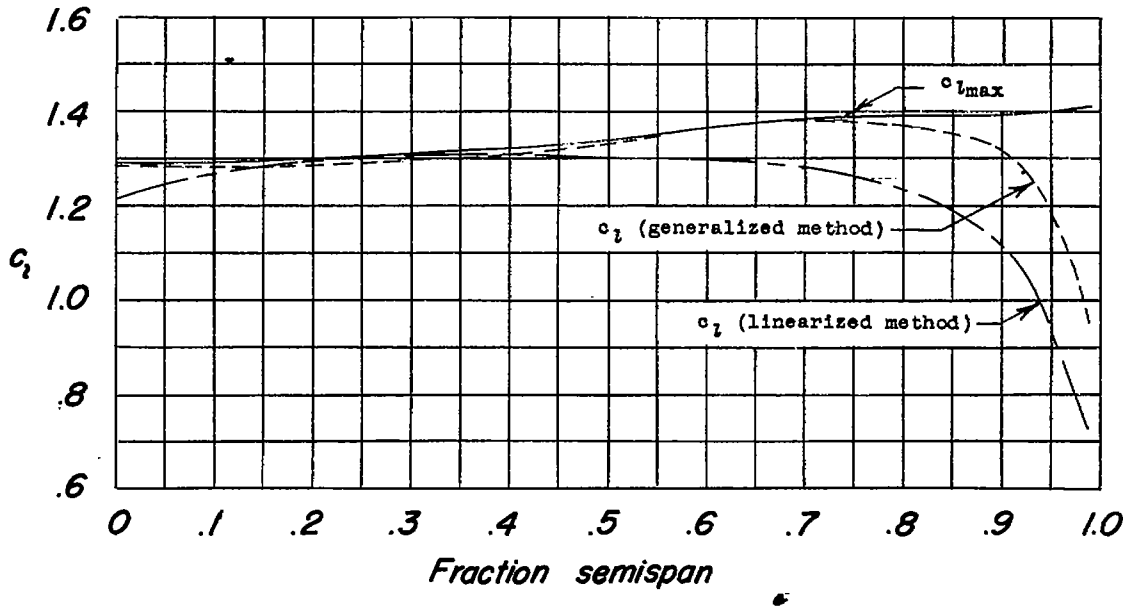

(a) Wing 2.5-12-44,24.

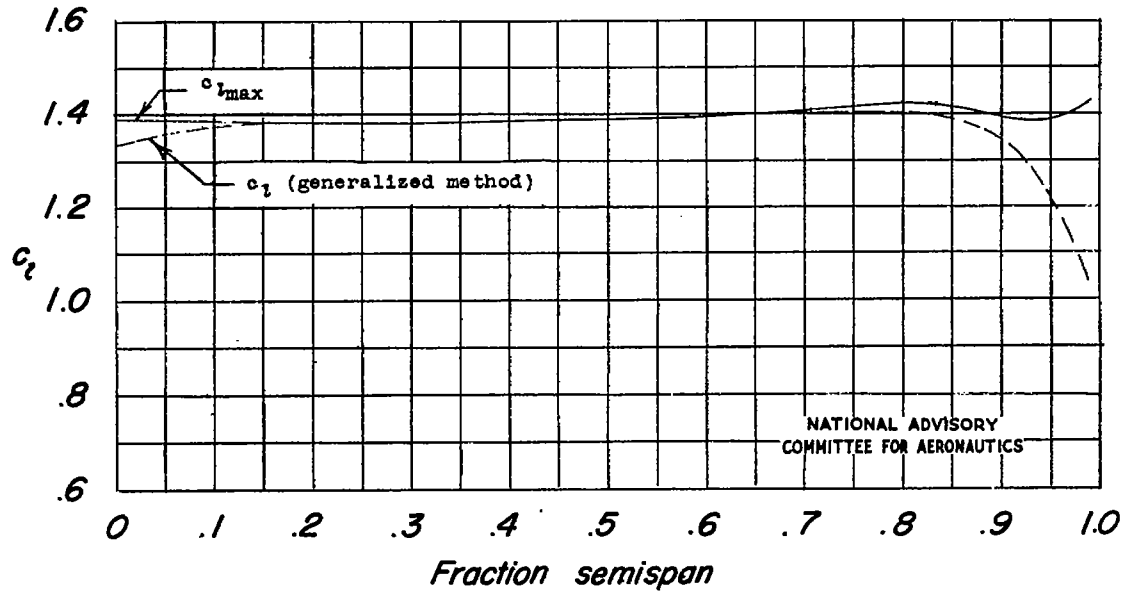

(b) Wing 3.5-12-44,22.1.

Figure 15.- Calculated distribution of c_l and $c_{l_{max}}$ over semispan at $C_{L_{max}}$.

TABLE I.- GEOMETRIC CHARACTERISTICS OF WINGS

Wing	Taper ratio	Aspect ratio	NACA airfoil		Span (ft)	Area (sq ft)	M.A.C. (ft)	Geometric washout (deg)
			Root section	Tip section				
2.5-8-44,16	2.5	8.04	4416	4412	15	27.994	1.990	4.5
2.5-10-44,20	2.5	10.05	4420	4412	15	22.393	1.592	3.5
2.5-12-44,24	2.5	12.06	4424	4412	15	18.661	1.328	3.0
2.5-8-44,24	2.5	8.04	4424	4412	15	27.994	1.990	2.4
3.5-8-44,14.7	3.5	8.03	4414.7	4412	15	28.021	2.070	3.0
3.5-10-44,18.4	3.5	10.04	4418.4	4412	15	22.418	1.656	3.0
3.5-12-44,22.1	3.5	12.06	4422.1	4412	15	18.656	1.382	3.0

NATIONAL ADVISORY
COMMITTEE FOR AERONAUTICS

TABLE II.- CALCULATED AND EXPERIMENTAL CHARACTERISTICS OF WINGS WITH SMOOTH LEADING EDGE

Wing	R	$C_{D_{min}}$			$(L/D)_{max}$			$\alpha_{(L=0)}$ (deg)		
		Calculated		Experimental	Calculated		Experimental	Calculated		Experimental
		Generalized	Linearized		Generalized	Linearized		Generalized	Linearized	
2.5-8-44,16	4.32×10^6	0.0080	0.0081	0.0090	29.4	28.8	27.8	-2.9	-2.8	-2.9
2.5-10-44,20	3.49	.0083	.0085	.0083	32.0	31.1	31.6	-3.0	-2.9	-3.2
2.5-12-44,24	2.87	.0088	.0087	.0091	32.6	32.6	33.4	-3.0	-3.1	-3.2
2.5-8-44,24	4.32	.0084	.0084	.0081	28.0	27.6	26.1	-3.1	-3.2	-3.2
3.5-8-44,14.7	4.00	.0076	------	.0074	29.8	----	29.5	-3.6	----	-3.4
3.5-10-44,18.4	4.00	.0080	------	.0082	32.4	----	31.1	-3.4	----	-3.5
3.5-12-44,22.1	4.00	.0081	------	.0088	33.9	----	33.0	-3.3	----	-3.5

Wing	R	$\frac{dC_L}{d\alpha}$			$C_{L_{max}}$			$\left(\frac{dC_m}{dC_L}\right)_{(L=0)}$		$C_{m_{(L=0)}}$	
		Calculated		Experimental	Calculated		Experimental	Calculated	Experimental	Calculated	Experimental
		Generalized	Linearized		Generalized	Linearized		Generalized		Generalized	
2.5-8-44,16	4.32×10^6	0.0823	0.0815	0 0820	1.48	1.42	1.54	0.007	0.012	-0.093	-0.099
2.5-10-44,20	3.49	.0827	.0828	.0860	1.41	1.36	1.43	.006	0	-.087	-.095
2.5-12-44,24	2.87	.0848	.0836	.0870	1.31	1.26	1.27	.016	.021	-.085	-.097
2.5-8-44,24	4.32	.0795	.0780	.0795	1.35	1.30	1.37	.014	.021	-.083	-.084
3.5-8-44,14.7	4.00	.0810	------	.0812	1.47	----	1.54	.008	.011	-.092	-.097
3.5-10-44,18.4	4.00	.0833	------	.0852	1.43	----	1.45	.008	.020	-.089	-.098
3.5-12-44,22.1	4.00	.0852	------	.0870	1.37	----	1.33	.015	.015	-.085	-.088

TABLE III.- CALCULATED AND EXPERIMENTAL CHARACTERISTICS OF WINGS WITH ROUGH LEADING EDGE

Wing	R	$C_{D_{min}}$		$(L/D)_{max}$		$\alpha_{(L=0)}$ (deg)		$\frac{dC_L}{d\alpha}$		$C_{L_{max}}$	
		Calculated (generalized)	Experimental	Calculated (generalized)	Experimental	Calculated (generalized)	Experimental	Calculated (generalized)	Experimental	Calculated (generalized)	Experimental
2.5-8-44,16	3.90×10^6	0.0129	0.0135	22.8	21.6	-2.7	-2.6	0.0778	0.0774	1.18	1.22
2.5-10-44,20	3.90	.0137	.0133	23.9	23.6	-2.6	-2.8	.0760	.0796	1.03	1.08
2.5-12-44,24	3.90	.0145	.0142	22.5	23.6	-2.5	-2.6	.0763	.0792	.88	.89
2.5-8-44,24	3.90	.0137	.0126	20.3	20.5	-2.6	-2.7	.0701	.0732	.91	.99
3.5-8-44,14.7	4.00	-----	.0112	----	23.0	----	-3.2	------	.0785	-----	1.26
3.5-10-44,18.4	4.00	-----	.0122	----	24.7	----	-3.2	-----	.0790	-----	1.10
3.5-12-44,22.1	4.00	-----	.0130	----	25.6	----	-3.1	-----	.0795	-----	.99

NATIONAL ADVISORY
COMMITTEE FOR AERONAUTICS

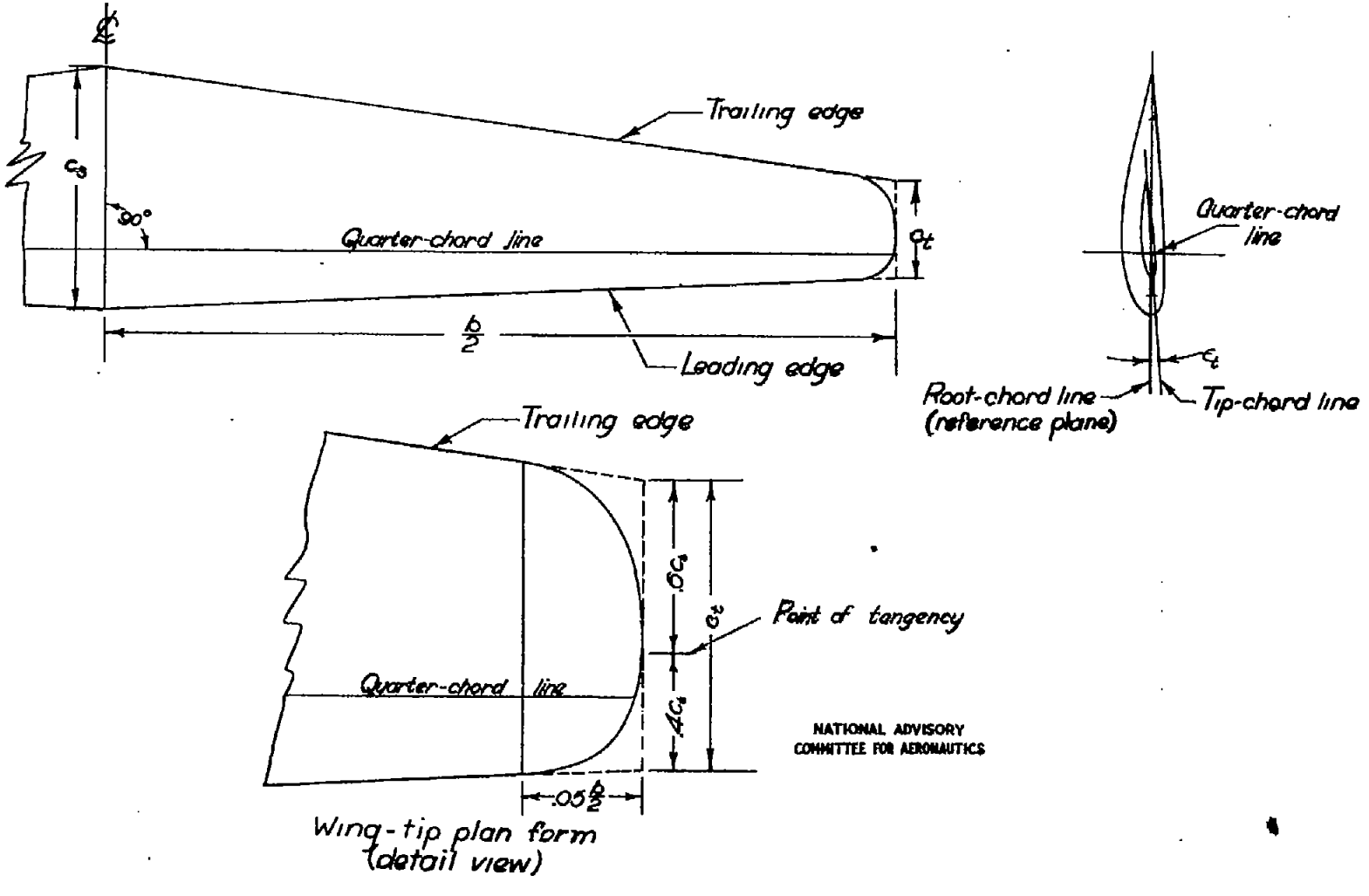

Figure 1.- Layout of typical tapered wing.

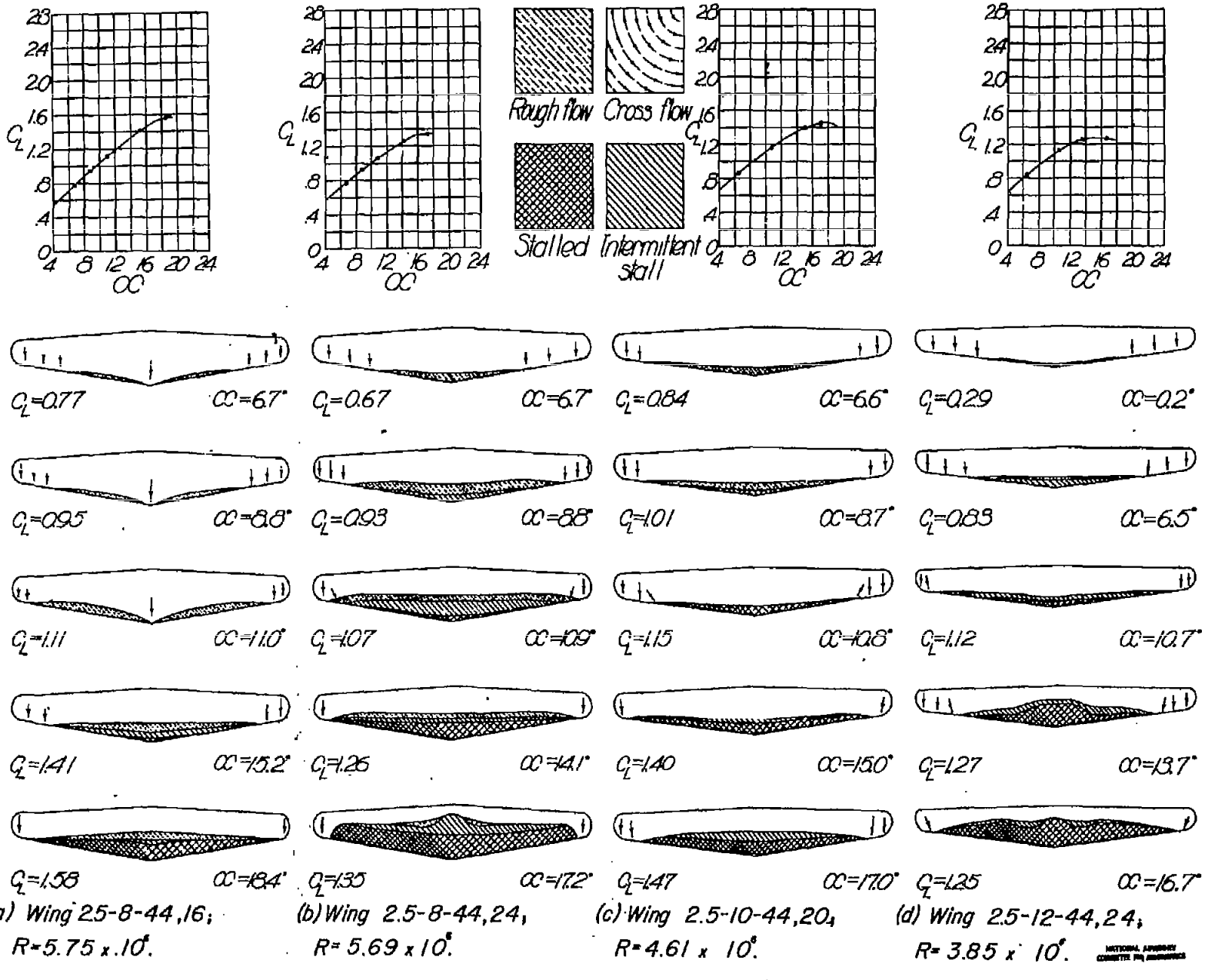

Figure 16.- Stall progression for wings of taper ratio 2.5.

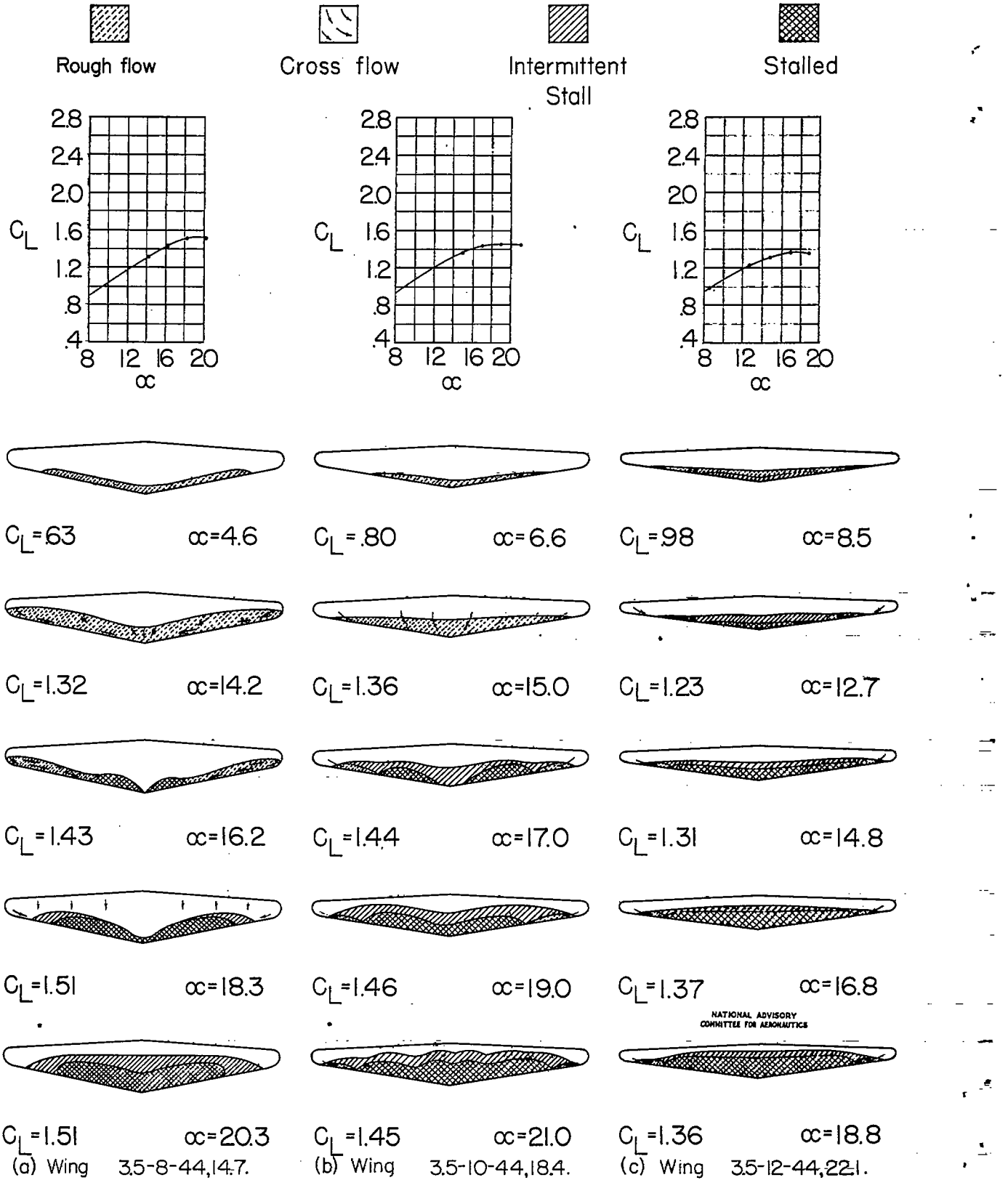

(a) Wing 3.5-8-44,14.7. (b) Wing 3.5-10-44,18.4. (c) Wing 3.5-12-44,22.1.

Figure 17.- Stall progressions for wings of taper ratio 3.5. $R \approx 4.0 \times 10^6$.

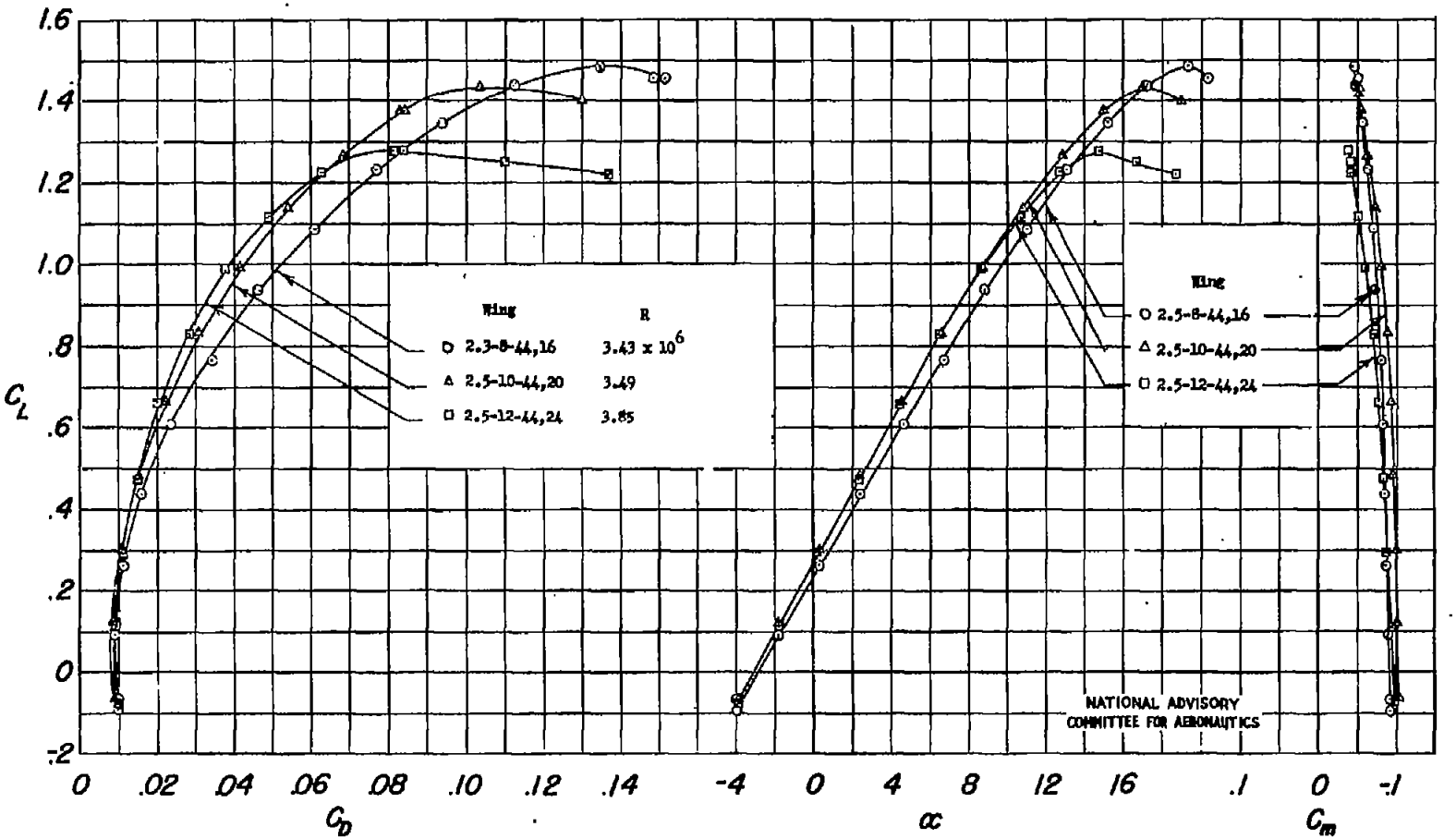

(a) Taper ratio 2.5; $R \approx 3.6 \times 10^6$.

Figure 18.- Effect of variations in aspect ratio and root thickness-chord ratio on characteristics of wings with smooth leading edge.

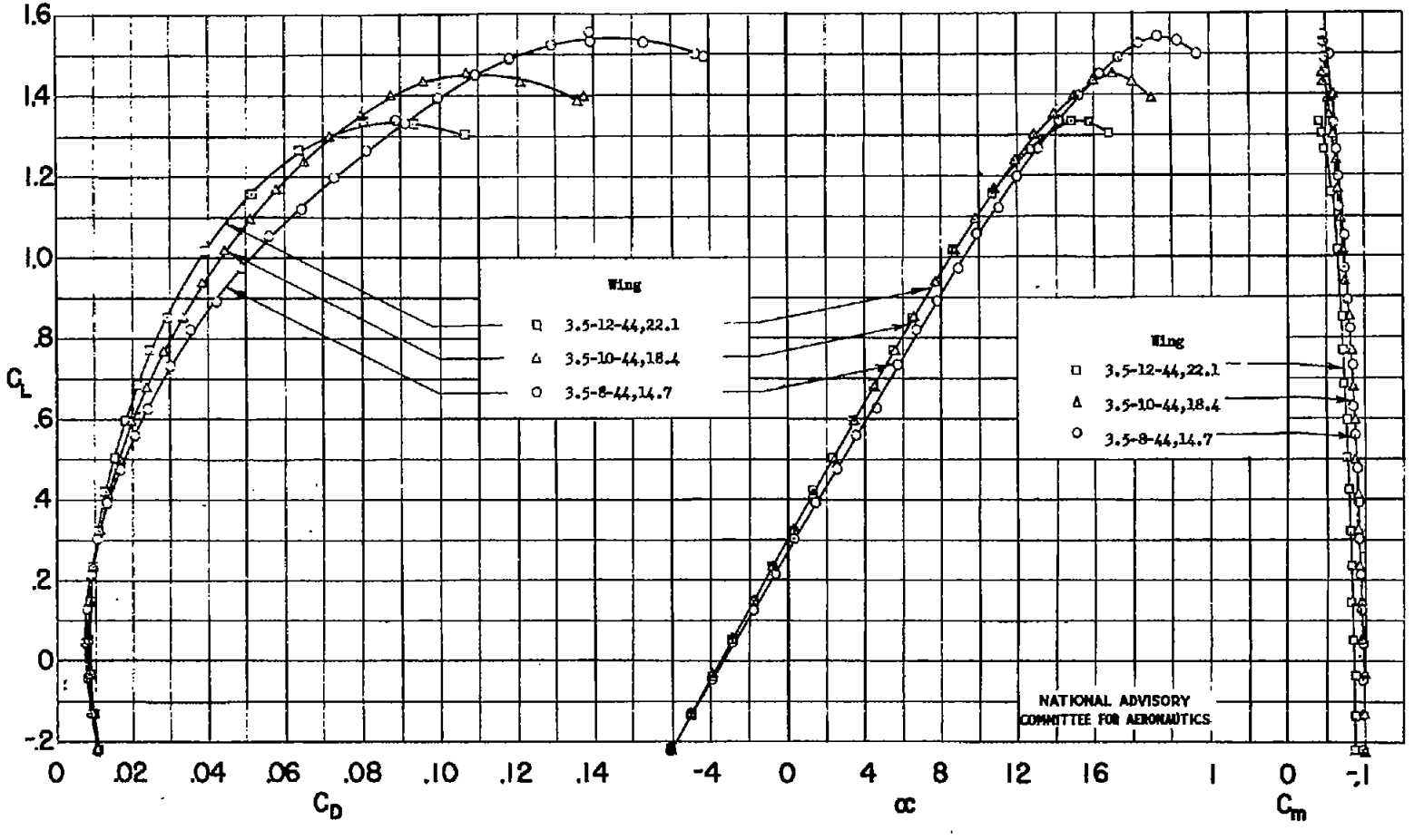

(b) Taper ratio 3.5; $R = 4.0 \times 10^6$.

Figure 18.- Concluded.

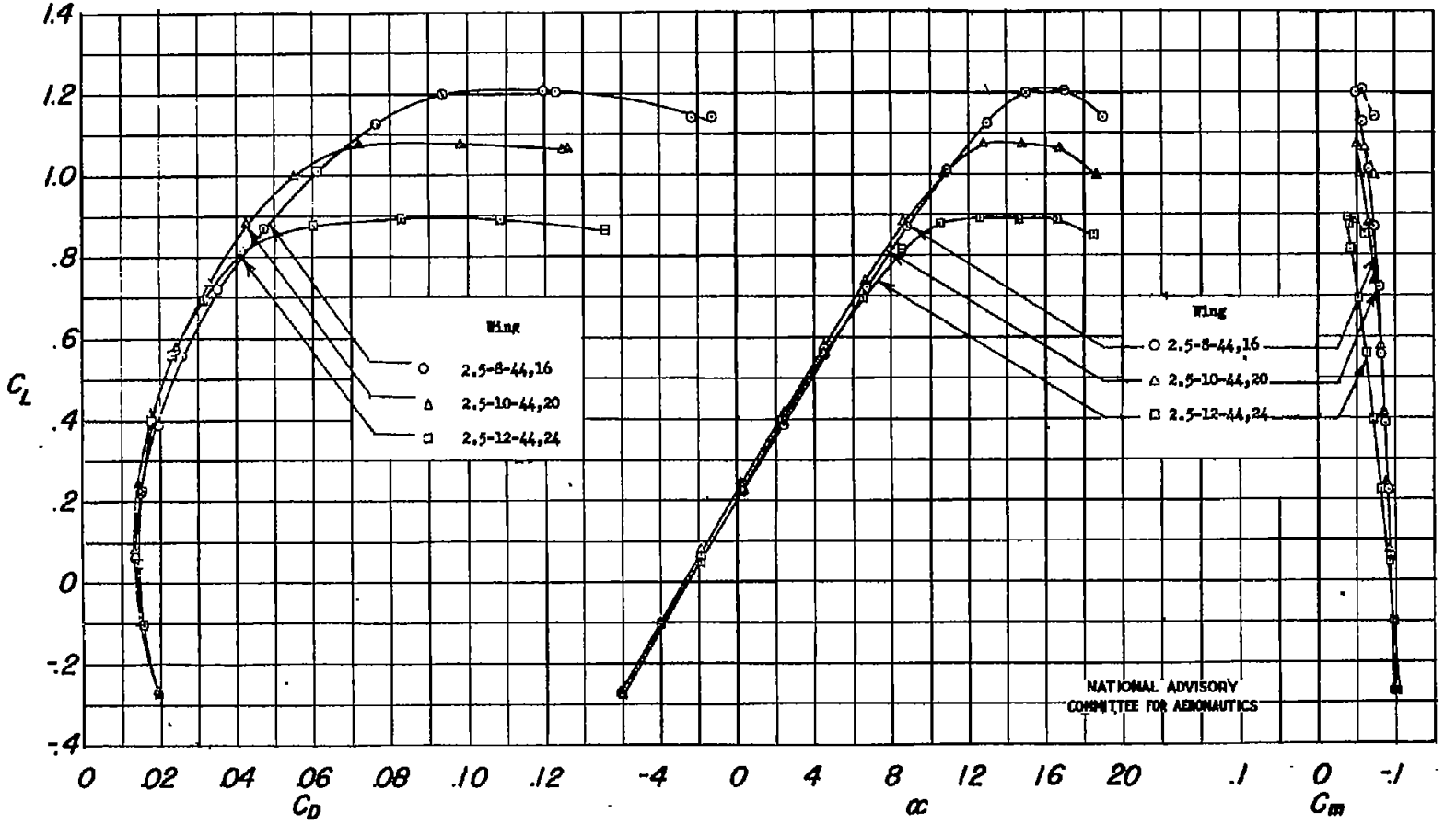

(a) Taper ratio 2.5; $R = 3.9 \times 10^6$.

Figure 19.- Effect of variations in aspect ratio and root thickness-chord ratio on characteristics of wings with rough leading edge.

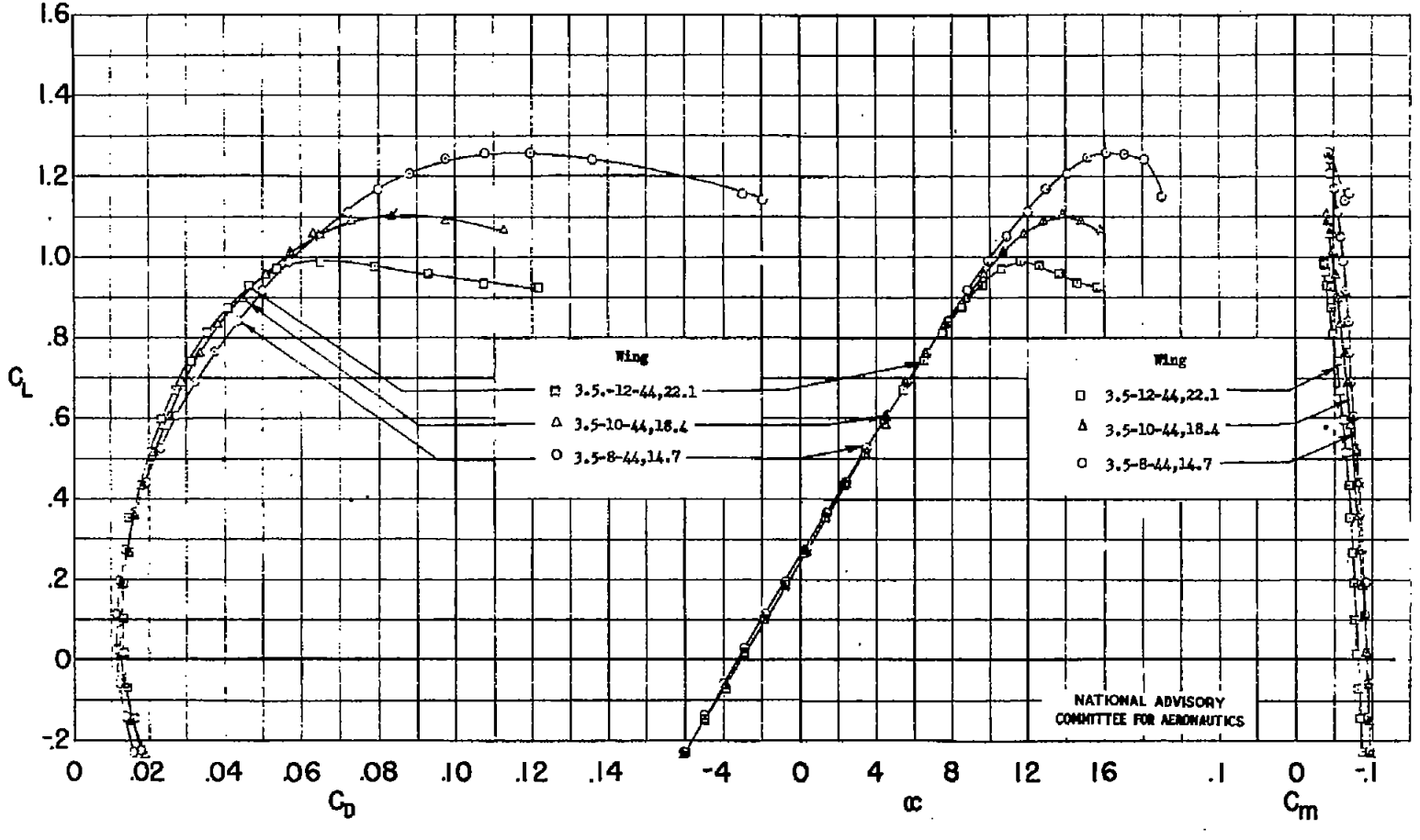

(b) Taper ratio 3.5; $R = 4.0 \times 10^6$.

Figure 19.- Concluded.

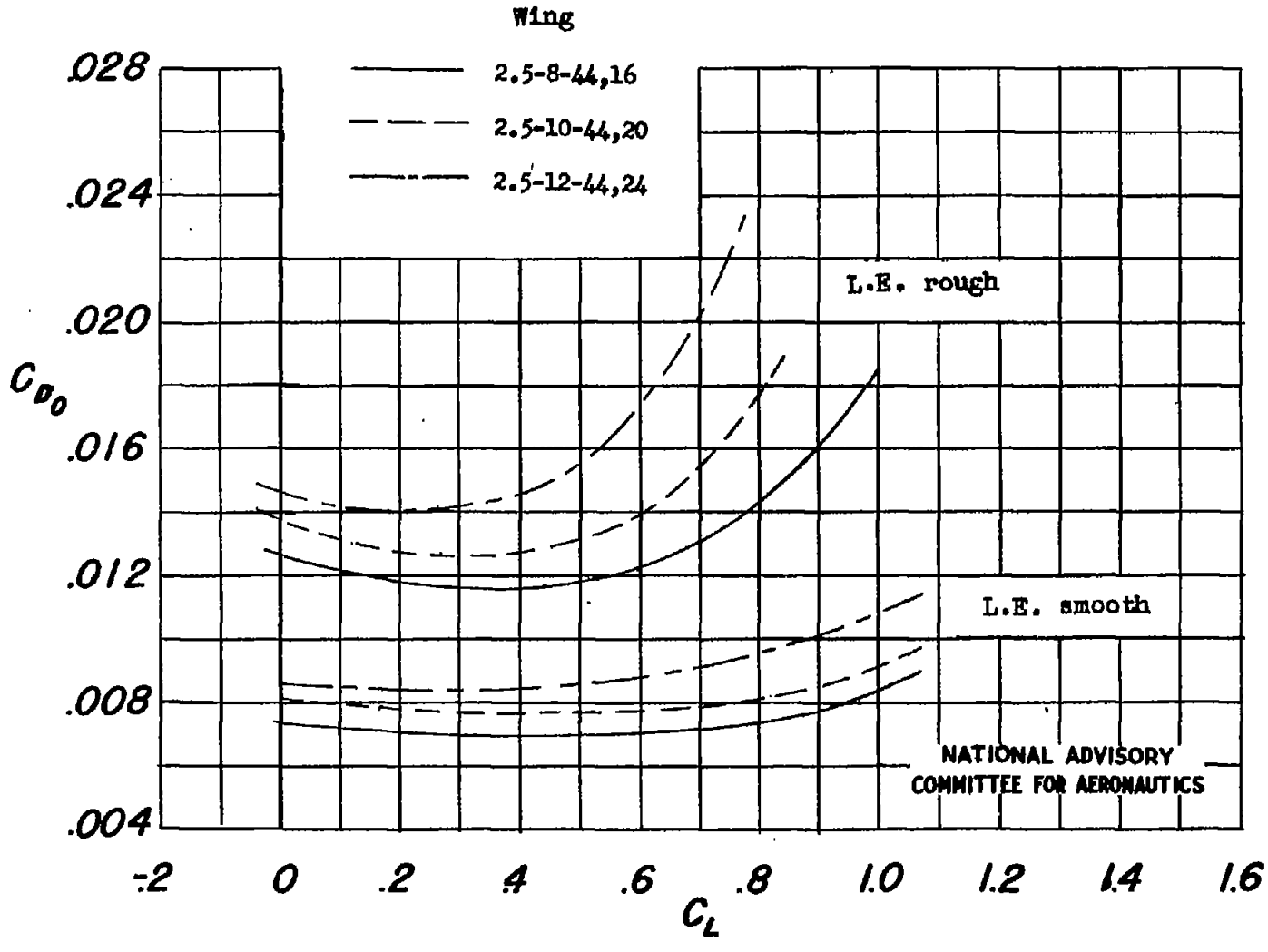

Figure 20.- Comparison of calculated profile-drag coefficients for smooth and rough wings.

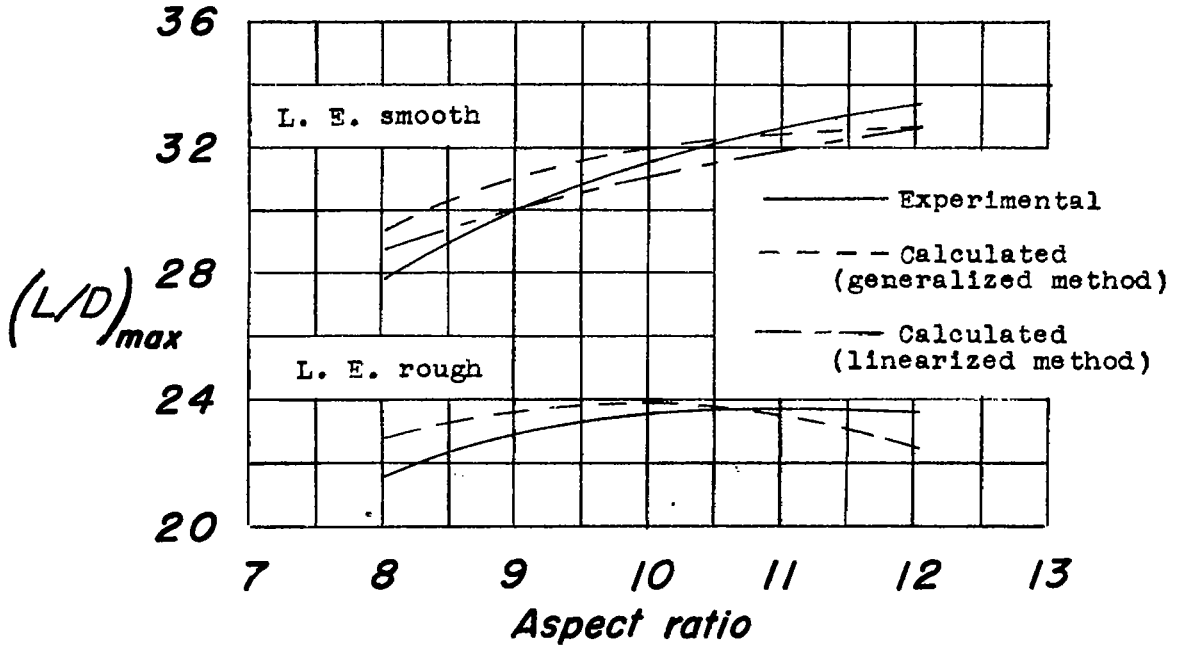

(a) Taper ratio 2.5.

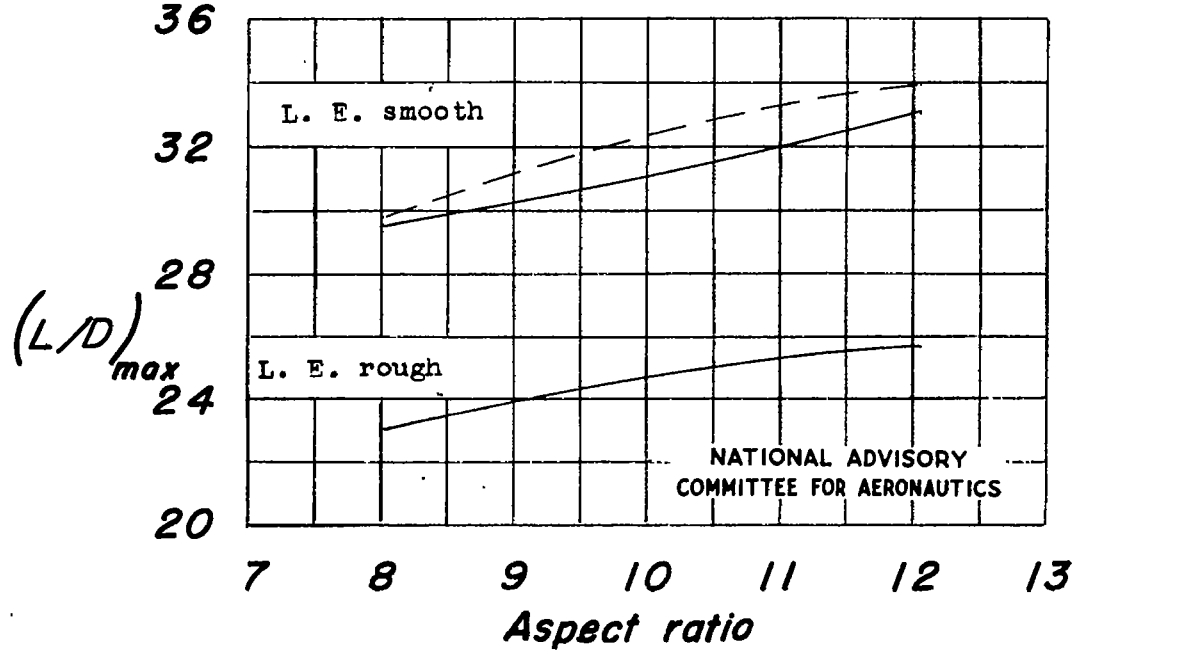

(b) Taper ratio 3.5.

Figure 21.- Variation of $(L/D)_{max}$ with aspect ratio. Ratio of span to root thickness, 35.

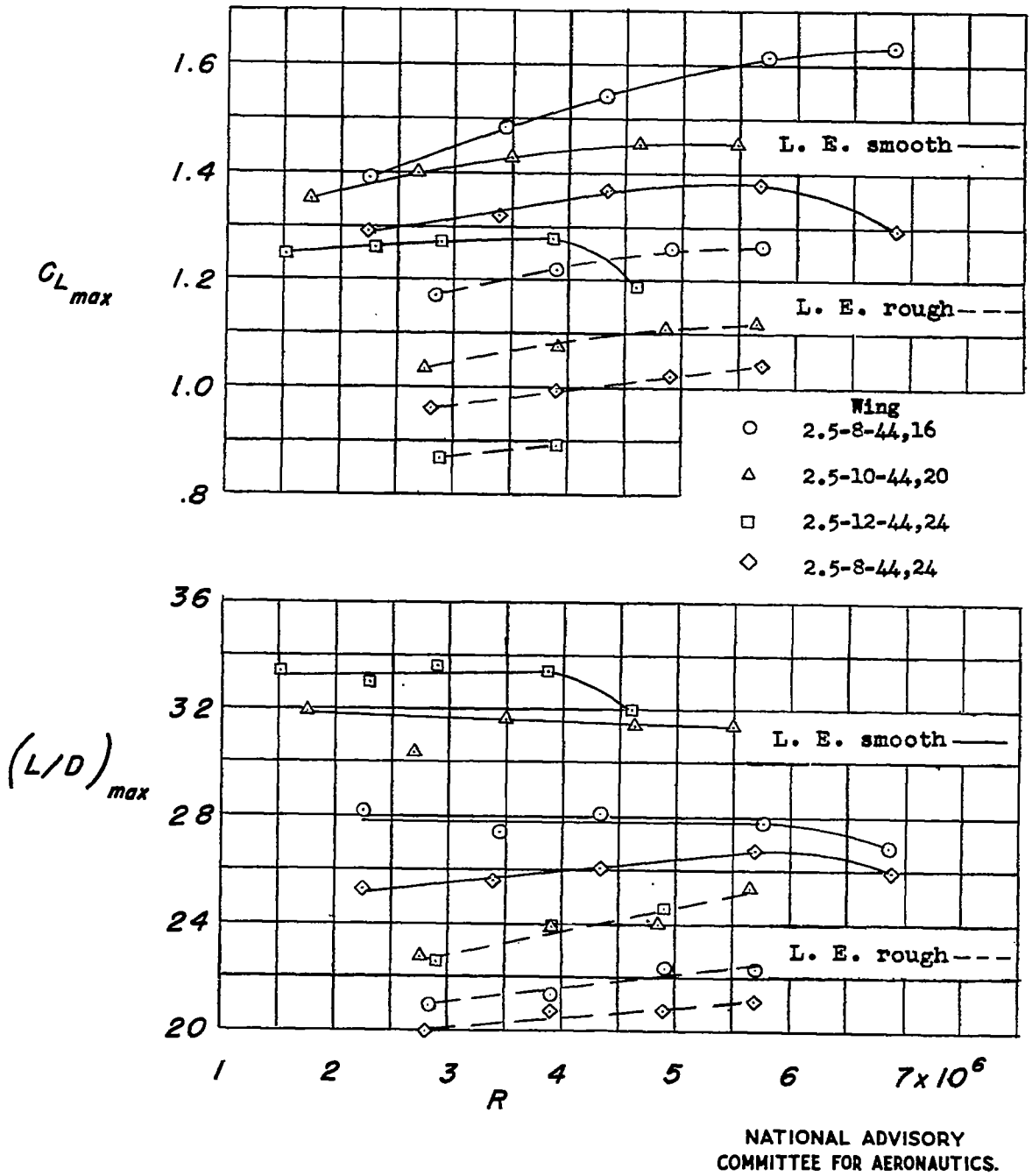

(a) Taper ratio 2.5.

Figure 22.- Effect of Reynolds number on maximum lift coefficient and maximum lift-drag ratio of a series of wings.

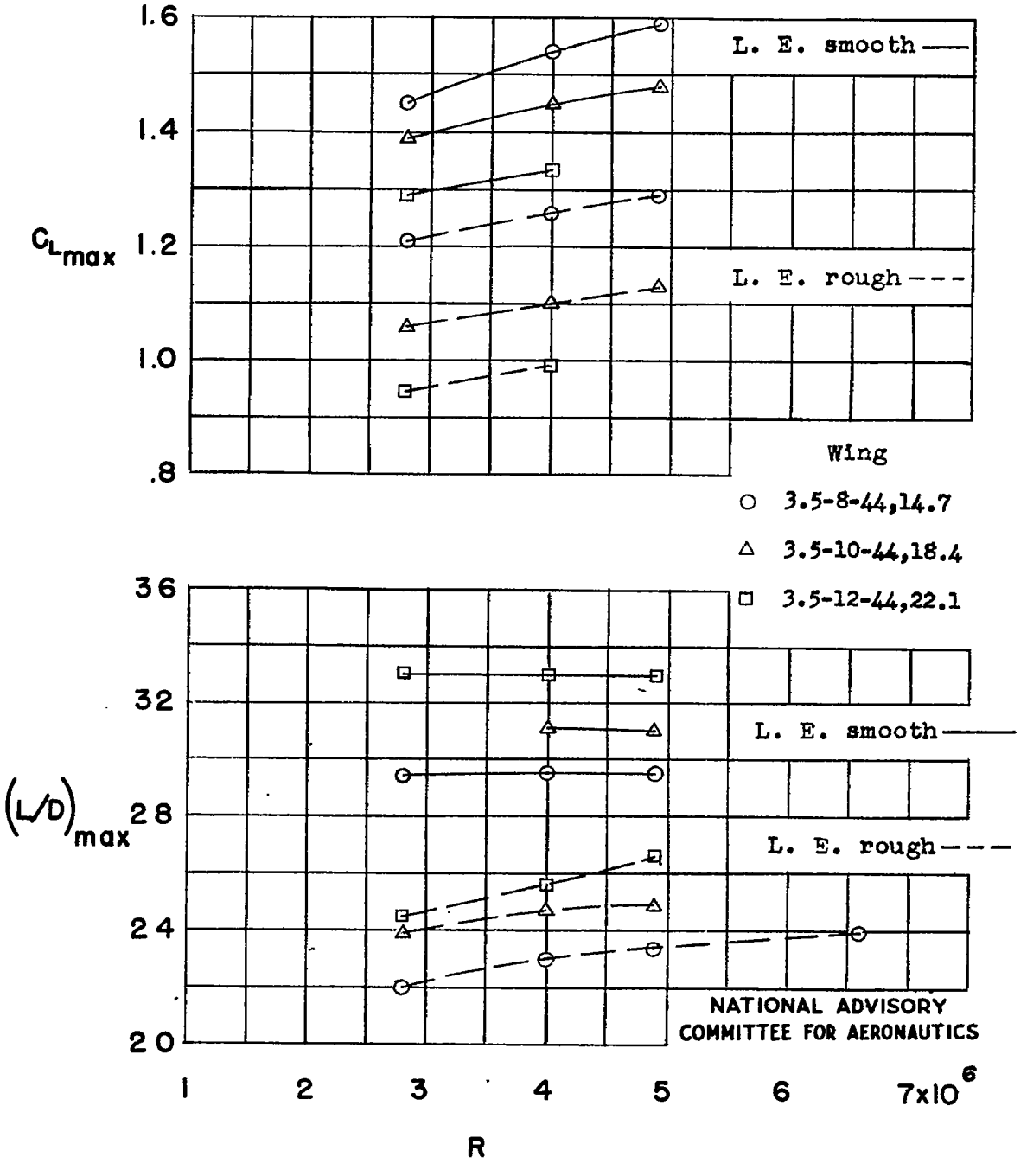

(b) Taper ratio 3.5.

Figure 22.- Concluded.